# Examining Kinetic and Thermodynamic DNA Destabilization Caused by the *cis-syn* Thymine Dimer Lesion Using Small Molecule Probes

by

Anne Malhowski

A thesis submitted to the Department of Chemistry of Mount Holyoke College in partial fulfillment of the requirements for the degree of Bachelor of Arts with honors

Program in Chemistry

Mount Holyoke College

South Hadley, MA

May 2005

This paper was prepared

under the direction of

Dr. Megan Núñez

for fourteen credits.

Table of Contents

List of Figures

# List of Tables

# Acknowledgements

I would first like to thank Megan Nunez, my thesis advisor. She has helped me so much throughout the course of my thesis research. Whenever I felt that my data didn't make any sense or when I had a rough day in the lab, she always made me feel like my project was amazing. Thank you, Megan, for all of your encouragement and great advice.

I would like to extend my thanks to all the people that helped me throughout my thesis research:

To the Nunez Lab Group: Amber Rosenberg, Catherine Volle, Aleksandra Mihailovic, and Amy Rumora. You all have been such an amazing support network for me. It's been a great two years working with you.

To the Mount Holyoke Chemistry Department and Christine Rowinski: The faculty at Mount Holyoke have helped me so much to mold me into the scientist that I have become.

To Lilian Hsu, thank you for letting me use the phosphorimager in your lab. I wouldn't have been able to run polyacrylamide gels without you.

To Darren Hamilton, if I couldn't use your lab's balance, I never would have able to measure so accurately. Thank you for the light box!

To Eric Girard, you are the Dry Ice King. Thank you for keeping the dry ice stocked for me so I could do all of my DNA reactions.

I would also like to thank Laura Khor, Amanda Socha, and Annie Yoon who always made sure that I never spent *too* much time in the lab.

To Amy Malhowski, my twin sister, you are the best sister a girl could ask for. You were there for me when things would go wrong or my research would get stuck. Thank you for listening to me and encouraging me.

To David Wagner, thank you for being my support when I needed you.

To my parents, David and Nancy Malhowski, who probably know way too much about my thesis research than they would ever like to know.

Thank you Mrs. DeGianfelice. If it was not for you, then I don't know if I would have found MHC or chemistry without you!

# ABSTRACT

DNA alternates through continuous cycles of mutation and repair. When DNA is exposed to UV radiation, adjacent thymines within a strand covalently link together, forming a cyclobutane ring through saturation of the 5, 6 double bonds. This lesion is known as a 6,4 *cis-syn* thymine dimer. Thymine dimers significantly perturb the structure of DNA by kinking the backbone by as much as 30 degrees. These helix-distorting lesions are bulky and can affect the binding of polymerases and sequence-specific proteins.

Repair of DNA lesions can proceed through two main pathways, base excision repair (BER), which repairs small lesions on DNA, and nucleotide excision repair (NER), which repairs large sequences of mutations. The BER pathway begins with an enzyme extruding the damaged base from the double-stranded DNA and then removing the mutated base by breaking the glycosidic bond to the sugar-phosphate backbone. After the excision of the base, the DNA can be reformed through repair synthesis of DNA and DNA ligation.

The process of how a mutation is repaired is understood; however, the process of how the enzyme finds the mutated base within the genome is still unclear. I hypothesized that damaged bases are kinetically and thermodynamically unstable, making them easier to find. I approached this problem using chemical probes to examine the mutation site and the bases around

the mutation. Information about the chemical accessibility of the adjacent bases could lead to a clearer picture of how an enzyme finds a mutation. Thus, base-specific reactions were used as chemical probes to examine bases around a thymine dimer mutation. Chemical probes include piperidine formidate, hydrazine, dimethyl sulfate, and potassium permanganate. Using chemical probes to examine the relative base reactivity of unmodified DNA and mutated thymine dimer DNA, quantitative results of DNA destabilization by a thymine dimer have been determined. In particular, the $KMnO_4$ probe, which reacts at only thymine bases, has produced significantly greater overall thymine reactivity on the thymine dimer DNA (AMM1 TT) in comparison to the unmodified DNA (AMM1). Using $KMnO_4$ to probe the complementary strand duplexed with AMM1 and AMM1 TT, the complementary strand duplexed with AMM1 TT was significantly more reactive towards the chemical probe than the AMM1 duplex. This result indicates that a thymine dimer-containing DNA strand makes a double helix more structurally destabilized. Through quantitative base destabilization research, more information can be obtained on the mutagenic characteristics, structural instability, removal and repair of DNA mutations.

# CHAPTER 1 - INTRODUCTION

Composed of simple bases, sugar, and phosphates, deoxyribonucleic acid, DNA, is the master structure from which information is coded to create and direct the process of life. In this paper, the importance of DNA structure and stability will be discussed in context of its environment, high fidelity replication ability, and repair mechanisms. The main focus of the paper will be on the topic of DNA mutations, which are the consequences when mistakes in DNA are not repaired. Of the mutations discussed, the concentration will be on the thymine dimer mutation—known to be the causal agent of skin cancer, and how past and present research have explored various methods in an attempt to quantify thymine dimer destabilization to the DNA double helix.

## 1.1 DNA Structure and Environment

DNA is the archive of genetic information in the form of nucleic acids, which consist of polymerized deoxyribonucleotides. A nucleic acid is composed of a base bound to the C1 carbon of a deoxyribose, which is in turn bound to a phosphate at the C5 carbon (Figure 1.1a). The polymerization reaction occurs between the C3 hydroxyl and phosphorus of the phosphate group on the C5 carbon, creating a phosphodiester bond. This reaction creates a string of nucleotides with an alternating sugar-phosphate backbone, which is highly negatively charged. The polymerized chains form an anti-parallel double helix,

meaning the 5' end of a strand is aligned with the 3' end of the other strand. The strands of the double helix are bound to each other through hydrogen bonding of Watson-Crick base pairs. The molecular composition of the bases allows guanine and cytosine to base pair, forming three hydrogen bonds, and adenine and thymine to base pair, which can form only two hydrogen bonds (Figure 1.1b). Inside of the helix, the bases pair to their complementary base perpendicular to the double helix axis. Stacking of the bases provides additional structural stability to DNA by the blending of base pi orbitals. The coil of the helix creates grooves in the DNA, the major and minor groove. The major groove is the side of the DNA bases that exposes the genetic information. Proteins mainly bind at the major groove because the DNA bases are more accessible (Nelson and Cox, 2004).

The structural integrity of DNA is dependent on the stability of its environment. Minor changes to the environmental conditions can have serious detrimental effects on the structure of DNA. Factors that affect the double helical character of DNA are sodium ion concentration, heat, and denaturant compounds. A decrease in sodium ion concentration and addition of heat can both result in the denaturing of the double helix into single strands. If DNA is heated to a temperature above its melting point, the hydrogen-bonding network will be disrupted, causing the strands to separate. Denaturants such as formamide are compounds that specifically disrupt the hydrogen-bonding network of the DNA, resulting in strand separation (Nelson and Cox, 2004).

A

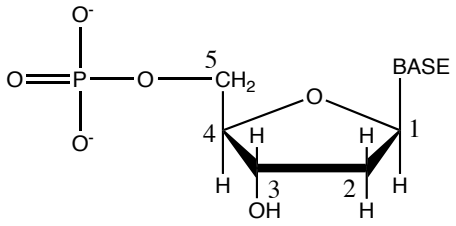


B

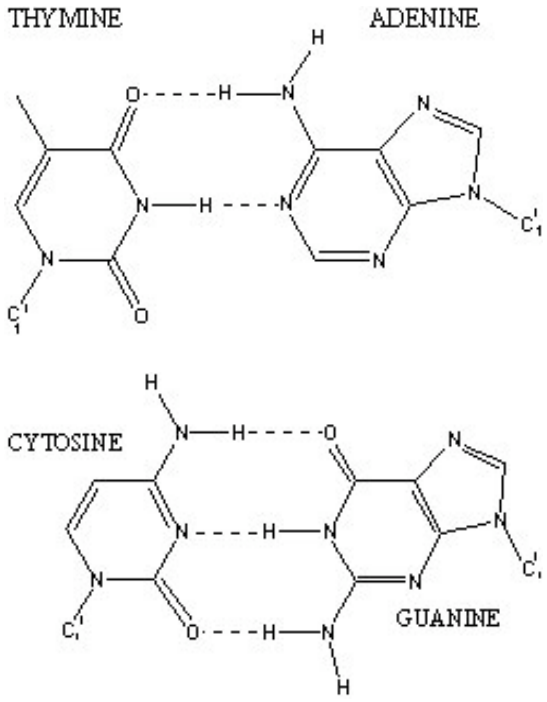


Figure 1.1 – *Chemical Structure of the Sugar-Phosphate Backbone of DNA (A) and Watson-Crick Base Pairing (B):* (A) The carbons in the deoxyribose sugar in DNA are numbered in a clockwise fashion, starting at the carbon that is bonded to the base. The phosphate group bonded to C5 is designated the 5' end of DNA and the OH group on C3 is the 3' end of DNA. (B) The Watson-Crick hydrogen bonds for GC and AT are designated as dashed lines between the hydrogen bond donor and acceptor atoms.

## 1.2 DNA Damage

DNA is in a dynamic state of constantly being mutated and repaired. DNA is commonly prone to mutation, occurring in replication, transcription, recombination, and even during repair. The long-term survival of an organism is dependent on genetic stability, and mutations that provide a positive effect are minimal. The maintenance of genetic stability requires high fidelity DNA replication and repair mechanisms for the lesions that continually occur in DNA. Most spontaneous mutations in DNA are temporary because DNA repair pathways immediately correct them: base-excision repair and nucleotide excision repair. Rarely do DNA repair processes fail to fix the mutation and allow DNA to be permanently altered. These mutations have been the cause of hereditary diseases, cancer, and even death (Alberts *et al.*, 1994).

## 1.3 Types of DNA damage: Endogenous and Environmental

DNA damage can fall under two main categories: endogenous and environmental damage (Figure 1.2). DNA undergoes major changes as a result of thermal fluctuations. Approximately 5000 purine bases are cleaved from the DNA in each human cell because of thermal disruption. Also, pH decrease can cleave the glycosidic bonds holding the base to the nucleotide, in a process known as depurination (Friedberg *et al.*, 1995). Spontaneous deamination of cytosine to uracil in DNA is estimated to occur at a rate of 100 bases per genome per day. The products of deamination, altered base pairs, can propagate further during

DNA synthesis (Alberts *et al.*, 1994). DNA bases are also subject to change by reactive metabolites such as oxygen radicals, which arise as byproducts from cellular respiration, can cleave the sugar phosphate backbone of DNA. One of the most common targets of oxidation is guanine, which is converted to 8-oxoguanine. 8-Oxoguanine can still pair with cytosine, but it prefers to base pair with adenine. The result of this mutation is evident in replication, which forms a base pair transition from GC to TA (Bruner *et al.*, 2000). Another type of spontaneous alteration in DNA includes tautomeric shifts, which are thought to be rare mutations, in which bases undergo bond rearrangement and form a structural isomer (Friedberg *et al.*, 1995). The main effect of this mutation is an alteration in the base-pairing properties of the mutated base. Besides endogenous DNA damage, exogenous environmental factors can also result in DNA damage. Factors such as ultraviolet light can promote a covalent linkage of two adjacent pyrimidine bases in DNA, creating thymine dimers. Most of these mutations lead either to deletion of one or more base pairs after replication or to a permanent base-pair substitution caused by mismatch propagation (Alberts *et al.*, 1994).

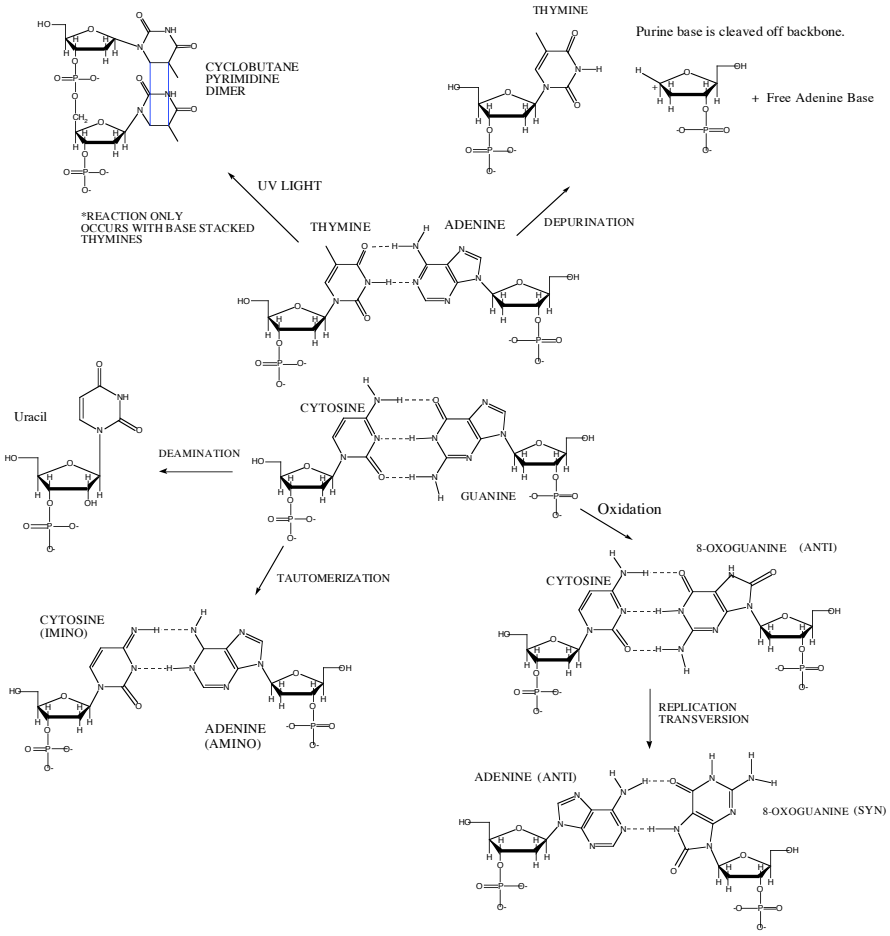


Figure 1.2: *Several Types of Endogenous and Environmental DNA Damage:* Depurination creates a strand break at the glycosidic bond. An 8-oxoguanine oxidation mutation, if not fixed before replication, can propagate into a transversion mutation. Tautomerization, which is rare, disrupts hydrogen bonding, which is designated by dashed lines. Deamination creates a transition mutation in which a cytosine is converted into a uracil base. Thymine dimers only occur between adjacent thymines, creating a cyclobutane ring at the C5, C6 double bonds of both thymines.

## 1.4 Thymine Dimer Mutation

Ionizing radiation and ultraviolet light are environmental sources for mutations. The energy from ionizing radiation such as gamma rays forms reactive ions and free radicals, which can be formed from water molecules and peroxide. UV radiation is less energetic than ionizing radiation but the bases of DNA absorb UV wavelengths to form detrimental mutations such as thymine dimers (Friedberg *et al.*, 1995).

UV radiation has been extensively studied and can be directly related to biological consequences in genotoxic effects of solar radiation prevalent in skin cancer. When DNA is exposed to radiation at wavelengths close to 260 nm, its absorption maximum, a variety of bases can be damaged, which can cause further mutation or result in cell death (Friedberg *et al.*, 1995). In particular, when UV light in the range of 200-300 nm irradiates adjacent thymines, these bases can covalently link together, forming a four-carbon ring through saturation of the 5, 6 double bonds (Figure 1.3) (Mees *et al.*, 2004). The [2+2] cycloaddition of two pyrimidines forms two major photoproducts: pyrimide-pyrimidone (6-4) photoproduct and *cis, syn*-cyclobutane pyrimidine dimer (CPD), which is the major product (Torizawa *et al.*, 2000). Thymine dimers significantly perturb the structure of DNA by causing the backbone to bend with a degree of distortion to B-DNA in the range of 7-30 degrees. (Figure 1.4) (Park *et al.*, 2002 and Brown *et al.,* 1986) These helix-distorting lesions are bulky and can affect the binding of sequence-specific proteins and also can prevent DNA replication.

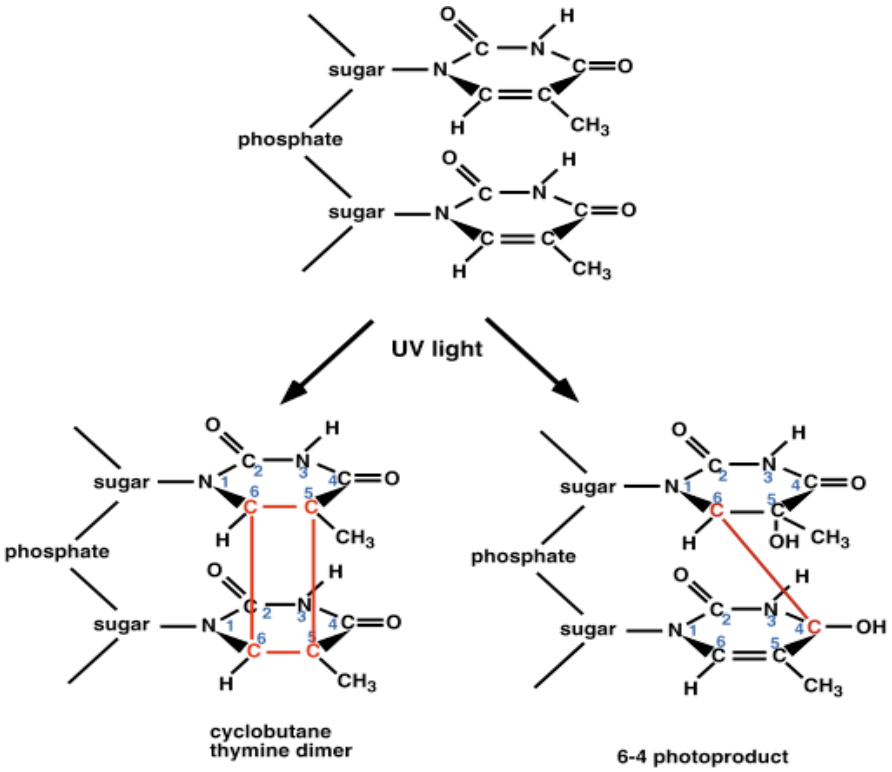


Figure 1.3 – *Products of Cycloaddition of Adjacent Thymines:* These dimers are both formed through covalent interactions between two adjacent pyrimidines located in the same polynucleotide chain. Through the saturation of the 5, 6 double bonds both of these products can form. (Picture used from http://www.public.asu.edu/~iangould/reallife/thymine/thymine.html)

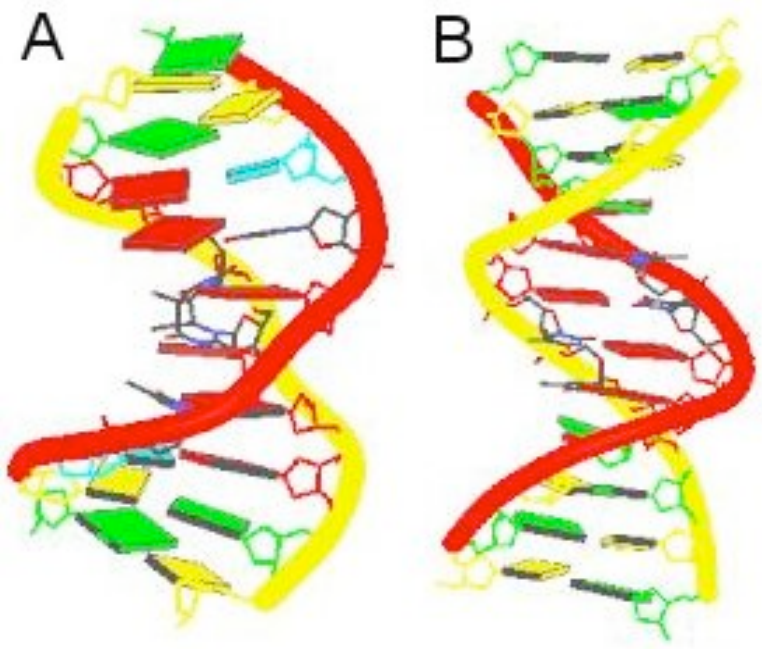


Figure 1.4 - *B-DNA with and without a Thymine Dimer:* (A) This is a picture of thymine dimer in B-DNA, which can be seen in the middle of the DNA as two adjacent red bases that have cyclized. The DNA is noticeable deformed from the dimer. (B) This is a picture of B-DNA without any DNA mutations in its stable conformation. (Adapted from Park *et al*. and Brown *et al.*)

## 1.5 Mutagens

Mutagens are natural or man-made chemicals that modify DNA bases. Some DNA base analogs such as bromouracil and aminopurine mimic the DNA bases and form point mutations in DNA. Mutagens can also be chemicals such as methanesulfonate, which is an alkylating agent, that create mispairing between bases. Intercalating agents such as ethidium bromide are considered mutagens because they insert between DNA bases, causing the DNA polymerase to insert an extra base across from the intercalating agent (Friedberg *et al.*, 1995 and Lewin, 2000).

## 1. 6 The Effect of DNA Mutations on Melting Temperature

DNA mutations range in their extent of DNA structural destabilization from minor energy alterations in the form of DNA mismatches to substantially change the melting point of the DNA duplex, which can be seen in thymine dimer mutations. The melting point for each DNA double helix is different and the length of the strand, percentage of GC base pairs, and base stacking all contribute to increasing the melting point. DNA melting is the loss of the double helical secondary structure, which exposes its internal single-stranded primary structure to solution, which can be measured by UV absorbance. UV absorbance of a DNA sample increases as the duplex is melted and the $T_m$ is the temperature at which the DNA is halfway between being single-stranded and double-stranded. $T_m$ is directly correlated to DNA stability and greater $T_m$ equates to greater DNA

stability (Rouzina and Bloomfield, 1999).

DNA structure has marginal stability under physiological conditions, meaning that the free energy transition between secondary and primary structures is very small. Even moderate changes in environmental conditions can shift the equilibrium between its double and single-stranded states. The formation of a DNA double helix has a large negative enthalpy and large positive entropy. The enthalpy term is favorably negative due to the electrostatic properties of DNA, which include hydrogen bonding and base stacking. The entropy term is large and positive due to the lack of solvation of bases and restriction of bond rotations for DNA in its double-stranded helical form. Thus, hydrogen bonding within a duplex is unfavorable entropically, but the enthalpic gain from the formation of many hydrogen bonds between the bases negates the entropic loss, making the helical form of DNA more favorable (Rouzina and Bloomfield, 1999).

In the case of DNA mutations, the balance between enthalpy and entropy is disrupted. For example, the thymine dimer lesion has been determined to destabilize DNA structure because the kinked backbone DNA disrupts base stacking and hydrogen bonding. The Lingbeck group studied the thermodynamic properties and melting points of a CPD-containing duplex and a *cis-syn* cyclobutane dimer formed between the two thymines of a TCT sequence, in relation to their corresponding undamaged DNA duplexes. The adjacent dimer decreased the free energy of the DNA duplex formation by 1.5 kcal/mol and the $T_m$ by 6 ºC relative to unmutated DNA. The nonadjacent dimer was much more

disruptive to duplex formation, which had a $\Delta\Delta G = 4.0$ kcal and $\Delta T_m = -17$ ºC. (Lingbeck and Taylor, 1999). The nonadjacent CPD was the more destabilizing lesion because, while the overall net bond change is the addition of 2 bonds, forming a cyclobutane ring between adjacent thymines, the mutation severely kinked the DNA structure over the cytosine base. The bending of the DNA duplex causes hydrogen-bonding strain, which decreases the melting temperature and makes the duplex more susceptible to unwinding (Nelson and Cox, 2004).

## 1.7 DNA Repair Pathways

However, hope is not lost when DNA mutates. Various pathways in which DNA mutations can be fixed include base excision repair (BER), nucleotide excision repair (NER), mismatch repair, direct repair, and SOS response. The BER pathway is initiated by DNA glycosylases and the mutations are excised as free bases. DNA glycosylases are damage-site specific and extrude the mutated base designed for its active site from the double-stranded DNA. An example of a site–specific DNA glycosylase is uracil glycosylase, which only removes uracil bases from DNA. DNA glycosylase removes base mutations by flipping the base into its active site and then removing the mutation by breaking the glycosidic bond (Nelson and Cox, 2004). Excision of the mutation results in the formation of apurinic sites, where nucleotides lack a base. The apurinic sites are removed by a second enzyme called apurinic/apyrimidinic (AP) nuclease. AP nucleases nick the DNA backbone through hydrolysis of a phosphodiester bond, which

produces a 5' terminal deoxyribose-phosphate residue, which is a substrate for DNA polymerase to repair the missing base, which is then ligated by a DNA ligase (Friedberg *et al.*, 1995).

Structural studies of BER glycosylases have revealed a common recognition mechanism to find DNA base mutations. These mechanisms include enzyme-initiated DNA distortion and DNA bending to flip the damaged base for recognition within a base-specific enzyme active site. In Gregory Verdine's research, hOGG1 enzyme, which repairs only the 8-oxoguanine mutation (8-oxoG), makes extensive contacts with the complementary cytosine base. Appropriate base pairing between the 8-oxoG and cytosine allows for the removal of 8-oxoG. However, despite extensive research, the steps involved in finding damaged bases out of all the normal bases are still unclear. One proposed mechanism includes the repair enzyme scanning the DNA duplex until a damaged site is detected (David, 2005).

Mismatch repair fixes only DNA bases that have been matched to a wrong Watson-Crick base, such as a GT mismatch. DNA mismatch repair in *E. coli* is initiated by a MutSLH protein complex. G-T mismatch is recognized by MutS, while MutH cleaves the backbone near the mismatch. The guanine is removed by an exonuclease and repaired by DNA polymerase (Nelson and Cox, 2004).

NER, in contrast to BER, uses enzymes to remove oligonucleotide fragment mutations. Examples of mutations that would need to be excised by NER include alkylated DNA bases with large hydrocarbon chains and pyrimidine

dimers. In the NER pathway, when the repair enzyme finds a large lesion, the phosphodiester backbone of the mutant strand is cleaved on both sides of the mutation to remove the mutant oligonucleotides (Alberts *et al.*, 1994).

Direct repair fixes mutations on a small scale, similar to BER. However, in contrast to BER, direct repair fixes mutations without excising the base. An example of a direct repair enzyme is photolyase, which can be found in *E. coli*. Photolyase uses a flavin adenine dinucleotide cofactor to transfer an electron to the cyclobutane pyrimidine dimer, which breaks the cyclobutane ring and reforms unbound thymine bases (Nelson and Cox, 2004).

A more extreme repair pathway is called SOS response, which is activated by extensive DNA damage in the form of radiation and involves the expression of many genes whose products include repair functions (Lewin, 2000). This repair pathway is error prone and an emergency response to save the highly mutated cell (Nelson and Cox, 2004). All of these repair pathways work together to retain the genetic integrity of DNA in a mutagenic environment.

### 1.8 Past Research on Thymine Dimer Mutations

Past research on DNA base mutations implemented various techniques to attempt to quantify the extent of destabilization to the DNA structure. One particular research group, Park *et al*., investigated the relationship between the DNA structure and properties of mutated DNA containing a cyclobutane pyrimidine dimer (CPD), the most abundant product in thymine dimer synthesis.

This group examined the DNA structure using X-ray crystallography. The crystal structure was of a DNA decamer duplex with one CPD lesion at a resolution of 2.0 angstroms. The DNA in this structure had an overall helical axis bend of 30° toward the major groove and an unwinding angle of 9°. In comparison to unmodified B-DNA, the CPD-containing DNA showed widening of the major and minor grooves in both the 3′ and 5′ direction of the CPD. The thymine dimer lesion also caused base pairing parameters to accompany for the bending DNA. Park *et al.* states that the substantial differences in structure of the CPD-containing DNA in comparison to its unmodified form could cause repair proteins to recognize it (Park *et al.*, 2002). Yet, the exact reasons of how repair proteins find these lesions are still unknown.

Taylor *et al.* used NMR to examine conformational and base-paring information of the *cis-syn* thymine dimer mutation. The thymine dimer mutation caused changes in chemical shift in comparison to unmodified DNA. The base most affected by the dimer mutation was the adenine, directly opposite the 3′-T of the thymine dimer site. In their research, greater changes in chemical shift were noticed on the 3′-side of the thymine dimer, indicating greater structural distortion of the bases near the 3′ side. Taylor *et al.* also conducted Nuclear Overhauser Effect experiments on the thymine dimer containing DNA decamer. In the NMR structure, the thymines in the dimer twist in a left-handed direction, suggesting the dimer is in a puckered conformation and flexible (Figure 1.5) (Taylor *et al.*, 1990).

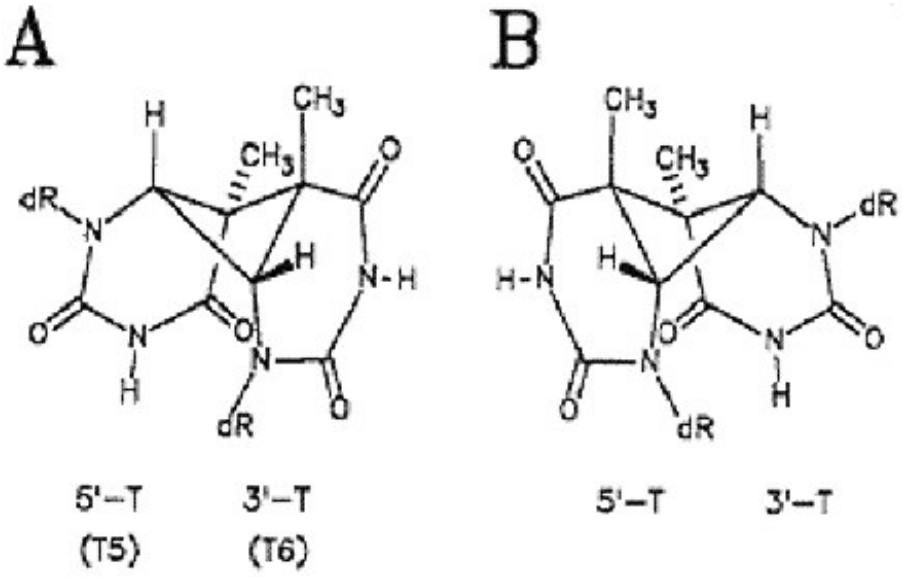


Figure 1.5 – *Thymine Dimer Conformations*: The cyclobutane ring of the *cis-syn* thymine dimer in a puckered conformation, according to the NOE data (A) and the 8-cyanoethyl phosphate derivative of the *cis-syn* dimer of dTpdT in the crystalline state (B). (Taylor *et. al,* 1990.)

Large upfield chemical shifts of the imino protons of the DNA duplex containing the thymine dimer indicate that the hydrogen-bonding network at the dimer and its paired adenines was weakened. However, it is not possible to conclude on the basis of imino proton chemical shifts alone to determine which hydrogen bonds of the dimer is weakened. The shifts could have caused changes in electronic structure of the thymines in the dimer or ring current effects, which occurs from dimerization (Taylor *et al.*, 1990).

Another common method of examining DNA lesions has been melting point determination. DNA melting indicates the temperature at which the base-pair hydrogen bonds break to unwind from the duplex state to the single-stranded state. Melting point determination for thymine dimers has indicated that in the presence of a thymine dimer lesion, the melting temperature decreases, which indicates destabilization of the overall DNA structure (Lingbeck and Taylor, 1999). According to the Taylor group, an unmodified DNA decamer duplex had a $T_m$ of 64 °C and a DNA decamer duplex containing a *cis-syn* thymine dimer had a melting temperature of 55 °C (Taylor *et al.*, 1990). This 9-degree drop in temperature has been considered to be only a slight perturbation of structure stability. Therefore, according to melting point determination, the thymine dimer mutation has been considered to slightly destabilize DNA structure. Thermodynamic data has shown insight into the overall structure of DNA; however, these tests still give little information about the structural stability of the individual bases around the mutation. The overall structure may not be perturbed

much, but the bases immediately flanking the thymine dimer could be more open to solvent contact and the base pairing could be strained. Alternatively, the base pairs at some distance from the mutation could unwind at a lower temperature range than the DNA duplex as a whole. However, this data simply cannot be extrapolated through thermodynamic data alone.

## 1.9 Probing of DNA Structure using Molecular Probes

The process of how a mutation is repaired is understood; however, the process about how the enzyme finds the mutation is still unclear. A new way of approaching this problem is using chemical probes to examine the mutation site and the base around the mutation to quantify DNA destabilization. Information about the adjacent bases could lead to a clearer picture about how an enzyme finds a mutation. Base-specific reactions could be used as chemical probes to examine bases around a mutation.

Some of the most well known molecular probing reactions are Maxam-Gilbert sequencing reactions, described in 1977 by Alan Maxam and Walter Gilbert. Maxam-Gilbert reactions are base-specific and modify at one particular base or a combination of purines or pyrimidines. The Maxam-Gilbert purine base reaction is a depurination reaction, which uses an acid piperidine formidate to cleave off the base (Figure 1.6) (Maxam and Gilbert, 1977).

In the C+T Maxam-Gilbert reaction, hydrazine adds to the 5, 6 double bond and then attacks the C4 carbonyl, which creates a new five-membered ring.

In the next step, piperidine is added, which yields the five-membered ring, two phosphates, and a deoxyribose fragment as products (Figure 1.7). While all of those reactions modify at a variety of bases, all of the reactions follow the same basic type of reactive process. These modifications, when reacted with piperidine, result in cleavage of the DNA backbone at the modified base. Examined through gel electrophoresis, the cleaved bases can be used to sequence a DNA strand (Maxam and Gilbert, 1977).

For the guanine reaction, dimethyl sulfate (DMS) methylates N7 of guanine (Nelson and Cox, 2004). Other bases are methylated but with the addition of piperidine at pH = 8 in the following step of the reaction, only the methylated guanines are cleaved (Figure 1.8). The leftover sugar groups are attacked by the C1 hydroxyl group, which opens the ring, and piperidine breaks the glycosidic bond, releasing the base (Bloomfield *et al.*, 2000).

Another DNA base modifier is potassium permanganate ($KMnO_4$), which oxidizes pyrimidine residues at the C5, C6 double bond and forms a *cis*-diol (Figure 1.9) (Ramaiah *et al.*, 1998). This base modifier could have trouble binding to a thymine dimer because the C5, C6 double bond has been cyclized to form a cyclobutane ring.

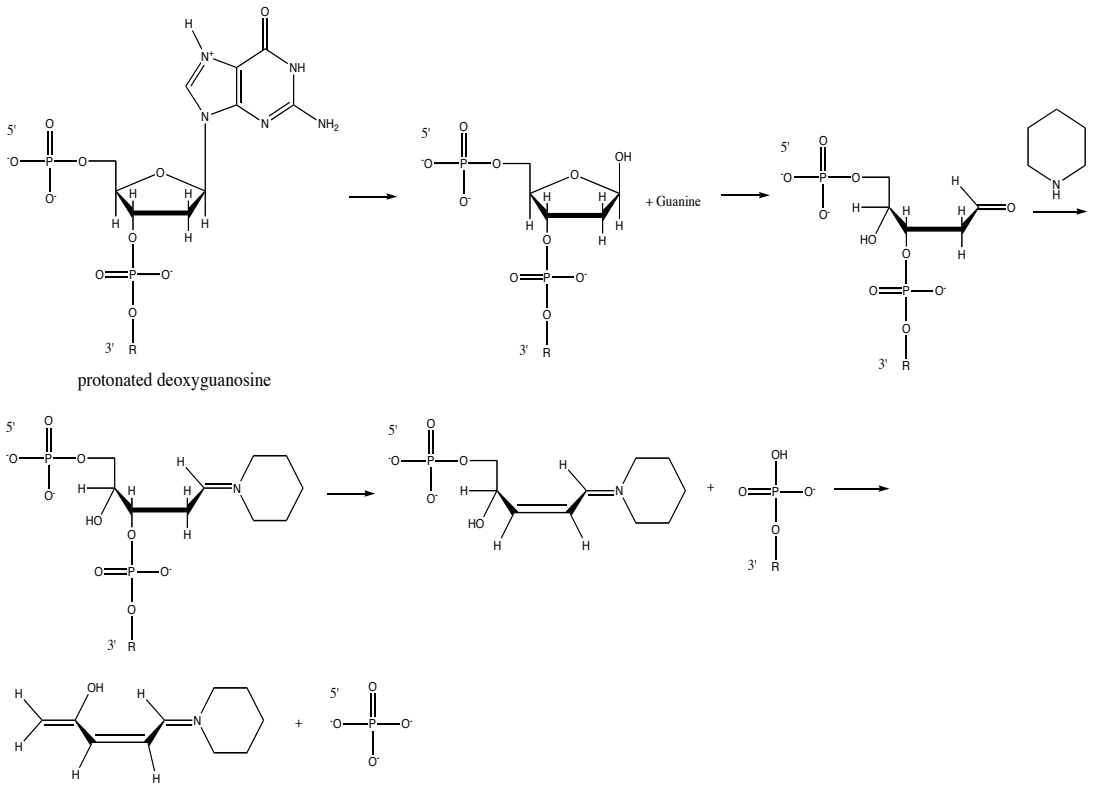


Figure 1.6 – *Maxam-Gilbert G+A Sequencing Reaction:* Piperidine formidate protonates the purine base at N7. Piperidine is added to cleave the sugar-phosphate backbone at the depurinated site (Nunez, 2004).

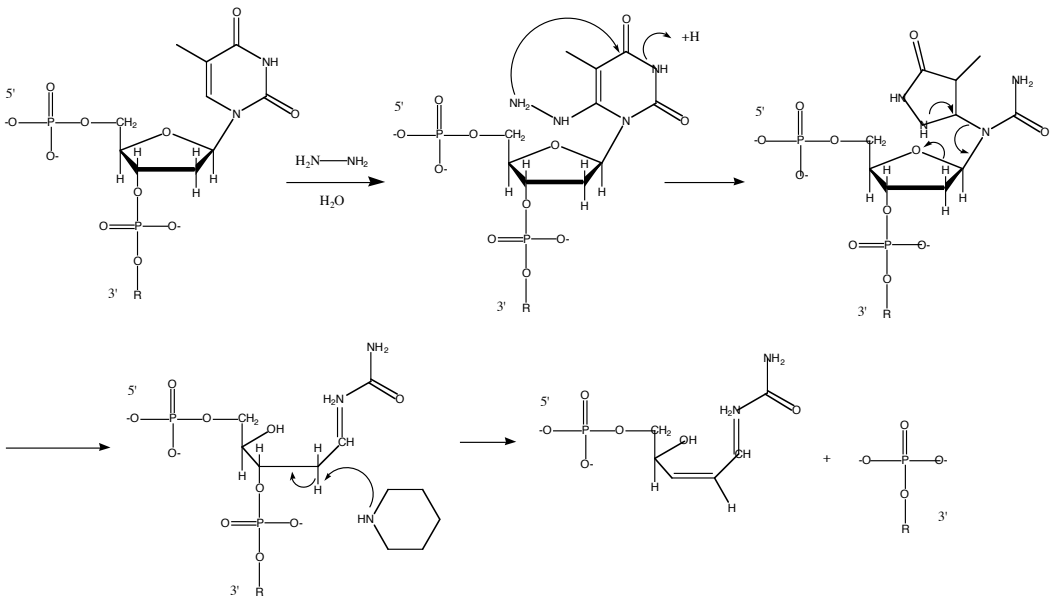

Figure 1.7 – *Maxam-Gilbert C+T Sequencing Mechanism*: Hydrazine attacks C6 of the pyrimidine base. Piperidine is added to cleave the sugar-phosphate backbone at the mutated base (Nunez, 2004).

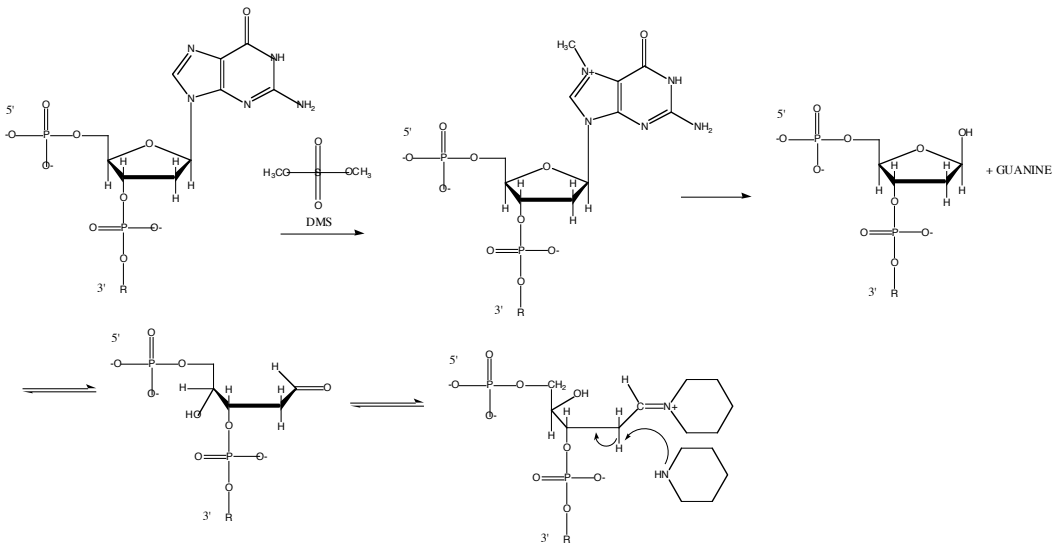


Figure 1.8 – *DMS Methylation Mechanism:* Dimethyl Sulfate (DMS) attacks guanines at N7. Piperidine is added to cleave the sugar-phosphate backbone at the mutated base (Nunez, 2004)

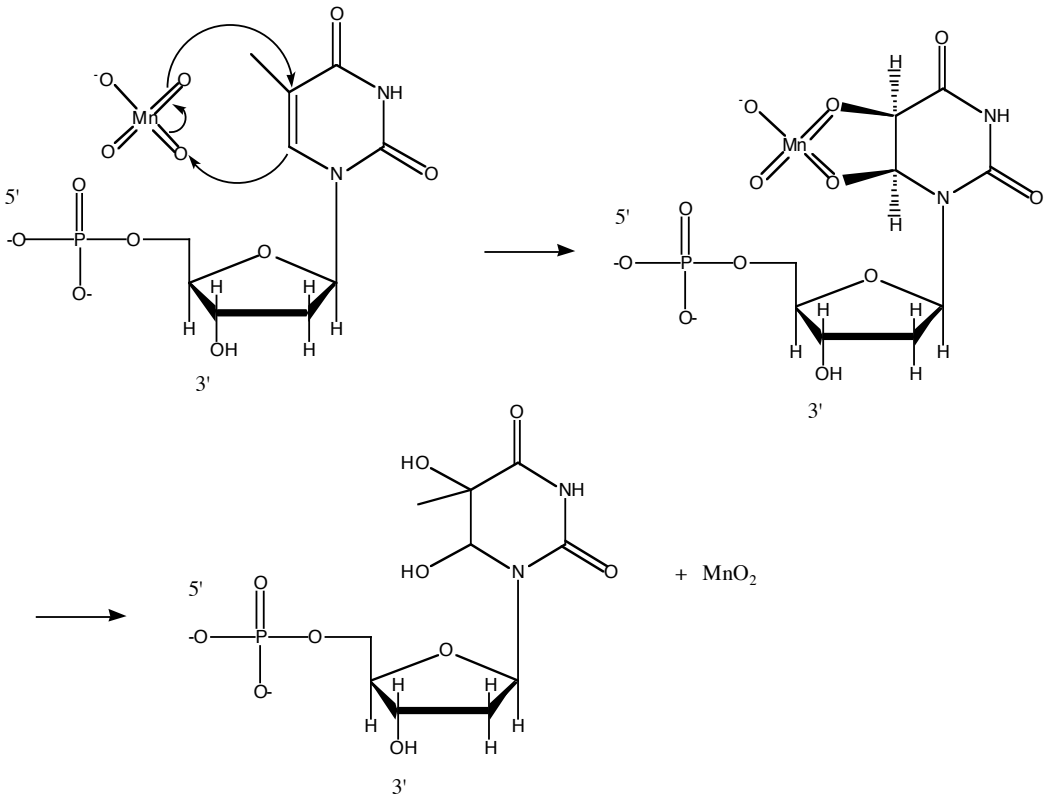


Figure 1.9 – *$KMnO_4$ Reaction with Thymine:* Permanganate attacks the C5, C6 double bond of thymine. (Figure adapted from Bruice, 1999)

## 1.10 Research Plan

The process of how a mutation is repaired is understood; however, the process of how the enzyme finds the mutated base within the genome, and the role of kinetic and thermodynamic destabilization in this process, is still unclear. This problem was approached using the chemical probes Maxam-Gilbert sequencing reactions for purines and pyrimidines, DMS, and $KMnO_4$ to examine the mutation site and the bases around the mutation. Information about the chemical accessibility of the adjacent bases could lead to a clearer picture about how an enzyme finds a mutation. Through quantitative base destabilization research, more information could be obtained on the mutagenic characteristics, structural instability, removal and repair of DNA mutations.

# CHAPTER 2 - EXPERIMENTAL METHODS

## 2.1 Deprotection and Cleavage of Synthetic Oligonucleotide from Solid Phase Resin for Single Strand DNA (AMM1) and its Complementary Strand (AMM2)

One μmol synthesis of a 19-mer DNA oligonucleotides, AMM1, and its complementary strand, AMM2, were obtained commercially from Integrated DNA Technologies (Figure 2.1). Both oligomers were specifically designed 19 base pair sequences, which had only one set of adjacent thymines in the AMM1 strand. The AMM1 and AMM2 oligonucleotides were synthesized using solid-phase phosphoramidite chemistry. Therefore, before chemistry could be done on the DNA, it had to be deprotected and cleaved of the controlled-pore-glass (CPG) resin. First, 1 μmol of each synthetic DNA strand was incubated with 800 μL of concentrated $NH_4OH$ for 6 hours at 55 ˚C, with occasional vortexing. After incubation, the tubes of DNA were cooled in the refrigerator and then put in a centrifuge briefly to pellet the resin. Then the solution was decanted and dried using a heated speedvac under vacuum. The dimethyoxytrityl group (DMT) was cleaved from the 5′ end of the DNA strands by incubation in 200 mL of 80% acetic acid for 15 minutes. Then, 800 μL of 100% ethanol was added and the samples were dried in the speedvac.

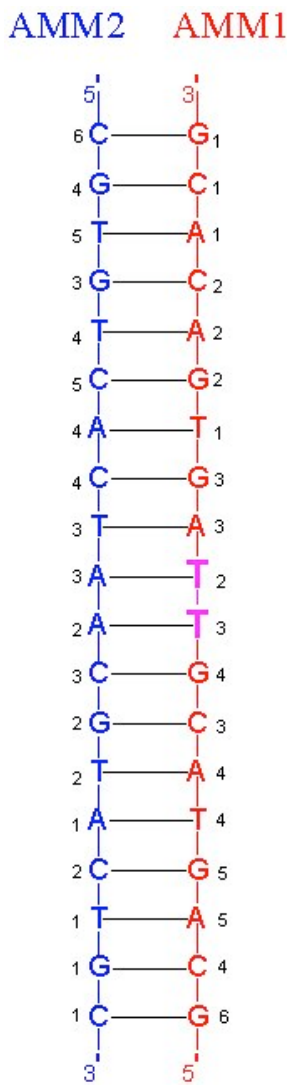


Figure 2.1 – *DNA Sequences of 19 Base Pair AMM1 and AMM2 Oligonucleotides:* The AMM1 sequence is red and the adjacent thymine, which was synthesized to become a thymine dimer, is bold and pink (T2 and T3 on AMM1). The complementary strand, AMM2, is blue. Each base is numbered in increasing order from the 3' ends of AMM1 and AMM2, according to the type of base.

2.2 Purification of single-stranded DNA (AMM1) and its complementary strand (AMM2) through Reversed-Phase HPLC

To prepare for injection into the HPLC, the DNA strands were resuspended in 200 µL 1X TE (Tris-HCl pH = 7.5 and EDTA pH = 8) and filtered in micro-filter tubes. AMM1 and AMM2 were purified using reversed-phase HPLC. See Table 2.1 for HPLC gradient for purifying the oligonucleotides. A C-18 reversed-phase column was used at a flow rate of 4 µL/min. Fractions of purified AMM1 and AMM2 were freeze-dried using a lyopholizer.

2.3 Synthesis of Thymine Dimer from Single-Stranded DNA (AMM1)

Approximately 2.4 mg of AMM1 was collected from the HPLC. Freeze-dried AMM1 was resuspended in 1 mL of 0.1 M sodium phosphate buffer (pH = 7.4). Of the total 2.5 mL AMM1, 1.25 mL was put into an Eppendorf tube with 25 mM of acetophenone (3.66 µL). The AMM1 DNA/acetophenone mixture was syringed into the round-bottom compartment of the vacuum-cuvette complex. The contents were frozen with liquid nitrogen and then put under vacuum for 5 seconds. Then the complex was purged with nitrogen gas and the frozen mixture was thawed. The freeze-pump-thaw process was repeated 4 times to purge oxygen from the system. When the sample melted for the last time, the sample was transferred into the quartz cuvette compartment. Then the AMM1/acetophenone mixture was irradiated in a UV light chamber ($\lambda$ = 300nm) for 3 hours.

Table 2.1 – HPLC Gradient for Purification of AMM1 and AMM2

| Time (min) | % acetonitrile | % 25 mM ammonium acetate |
|---|---|---|
| 0 | 5 | 95 |
| 5 | 5 | 95 |
| 25 | 10 | 90 |
| 30 | 5 | 95 |

Table 2.1 – AMM1 eluted at 15 min and AMM2 eluted at 19 min.

## 2.4 Purification and Separation of Thymine Dimer DNA from AMM1

After irradiation, the thymine dimer DNA (AMM1 TT) was purified using an Agilent 1100 series HPLC to remove any byproducts and unreacted AMM1. A series of gradients were used to find the best separation between AMM1 TT and AMM1. Despite the best of attempts, the two peaks could not be completely resolved. The gradient used for the dimer separation can be seen in Table 2.2. The injection size was 100 μL and the column used was the C-18 reversed-phase column. The collected purified AMM1 TT was freeze-dried in a lyopholizer.

## 2.5 Cycloreversal of AMM1 TT into AMM1

The thymine dimer is in equilibrium with unmodified thymine bases. Therefore, if the dimer was actually created then it could be cycloreverted back to its original state if reacted again in UV light to prove that a thymine dimer was synthesized. In this test, 350 μL of AMM1 TT and 1 mL of sodium phosphate buffer was mixed in the quartz cuvette and then irradiated in UV light for one hour. To see if the AMM1 TT reverted back into unmodified AMM1, three HPLC tests were done using the C-18 column at a flow rate of 4 μL/min. One HPLC run was pure AMM1 TT with an injection of 200 μL. Another run was pure AMM1 with an injection of 50 μL. The third run was a 200 μL injection of the cycloreverted DNA. The same gradient, which can be seen in Table 2.2, was used again to remain consistent with previous purification processes.

Table 2.2 – HPLC Gradient used for the Separation of AMM1 TT and Unreacted AMM1

| Time (min) | % acetophenone | % 25 mM ammonium acetate |
|---|---|---|
| 0 | 2 | 98 |
| 7 | 3 | 97 |
| 20 | 8 | 92 |
| 25 | 10 | 90 |
| 30 | 50 | 50 |
| 35 | 50 | 50 |
| 40 | 5 | 95 |
| 45 | 5 | 95 |

Table 2.2 - AMM1 TT eluted at 16.5-19.8 min and the unreacted AMM1 peak eluted at 20.4 min.

## 2.6 Electrospray Ionization Mass Spectrophotometry (ESI-MS) on AMM1 TT

To confirm that the thymine dimer was pure and at the correct length and sequence, its mass was determined using ESI-MS facilities at UMASS Amherst. AMM1 TT was resuspended to a concentration of approximately 10 picomoles per microliter in a solution of 50% methanol, 50% water, and 1% ammonia. Only 200 µL were used for the injection. The mode for the ESI-MS was set at negative ion mode, the gas pressure was 7 psi, the flow rate was 5 L/min, and the temperature was set at 250 ºC.

## 2.7 Radiolabeling of DNA at the 5′ end

The radioactive [γ - $^{32}$P] ATP was allowed to thaw on the 37 ºC heat block for approximately 20 min. While it was warming, AMM1 TT was resuspended in 100 $\mu$L 1X TE. One vial of freeze-dried unmodified AMM1 was also resuspended in 100 $\mu$L 1X TE. For each strand to be radiolabeled, the reaction mixture in Table 2.3 was prepared. The tubes were mixed gently, spun down briefly, and incubated at 37 ºC for one hour. Then 150 $\mu$L TE buffer, 100 $\mu$L of 7.5 mM $NH_4OAc$, and 750 $\mu$L 100% ethanol were added and the radiolabeled AMM1 TT and AMM1 were ethanol precipitated. The radiolabeled DNA was dried down and then piperidine treated.

Table 2.3 – Mixture for Radiolabeling DNA

| Material | Amount ($\mu$L) |
|---|---|
| DNA | 5 AMM1/ 10 AMM1 TT |
| Buffer for PNK | 5 |
| [$\gamma$ - $^{32}$P] ATP (30 mCi/mole) | 5 |
| PNK | 1 |
| $dH_2O$ | 34 |

Table 2.3 – The total reaction volume was 50 $\mu$L

*AMM1 TT was diluted for UV-Vis tests so the amount of AMM1 TT DNA was doubled for this reaction.

**Due to recurring low amounts of radioactive AMM1 TT, 6$\mu$L [$\gamma$ - $^{32}$P] ATP was added to the AMM1 TT reaction. More radioactivity increased the yield of radiolabeled sample.

2.8 Piperidine Treatment of DNA

Radiolabeled DNA, as well as the reactions discussed in the procedure sections 2.13 - 2.17, was reacted with piperidine to cleave any modified DNA strands. The cleaved radioactively-labeled DNA would then be able to be separated on a polyacrylamide electrophoresis gel. To each DNA sample, 100 $\mu$L of 10% piperidine was added and incubated for 30 min at 90 ºC. After incubation, the tubes were cooled, centrifuged, and dried in the speedvac. In order to ensure that all of the piperidine was expelled from the DNA samples, 20 $\mu$L of $dH_2O$ was added to each DNA sample and dried a second time in the speedvac.

2.9 Preparing Polyacrylamide Gels

The polyacrylamide solution was made from the components listed in Table 2.4. The polyacrylamide gel polymerized for 1 hour. When the gel was set up to run, 1 L of 1X TBE buffer (Tris-Borate and EDTA, pH = 8.3) was made to fill the bottom and top containers of the gel electrophoresis apparatus. DNA was resuspended in 1X blue running dye according to the radioacitve amount (CPM) in the DNA samples at 1 µL of dye per 10,000 CPM.

Table 2.4 – Polyacrylamide Gel Solution

| Material | Amounts for a 20% gel | Amounts for a 18% gel |
|---|---|---|
| Sol Gel concentrate | 96mL | 86.4mL |
| Sol Gel diluent | 12mL | 21.6mL |
| Sol Gel buffer | 12mL | 12mL |
| 10% ammonium persulfate | 600 $\mu$L | 600 $\mu$L |
| Temed | 30 $\mu$L | 30 $\mu$L |

Table 2.4 – After the concentrate, diluent and buffer were mixed together, the ammonium persulfate and TEMED were added to promote polymerization. The 20% gels were used for AMM1, AMM2, and AMM1 TT reactions to achieve the best separation. The 18% gels were used primarily for preparative gels to purify 5'-radiolabeled DNA for purification.

2.10 Purification of DNA recovered from a preparative polyacrylamide gel.

The radiolabeled DNA was detected by exposing film on the gel. The film was exposed for 5 minutes, soaked in developer for 3 minutes, and soaked in fixer for 3 minutes and then rinsed with water. The exposed spots on the film that were highest on the gel, which were the full length radiolabeled DNA, were cut out. Those gel pieces were crushed in 600-800 $\mu$L of 1X TE and the mixture was incubated at 37 ºC for several hours. After diffusion was complete, the supernatant was removed and filtered using micro-filter tubes. For further purification, the DNA was run through a Nensorb 20 cartridge column to remove borate, urea, and any remaining gel pieces. The column was prepped with methanol and 1X TE. Then the sample was added and the liquid was pushed through the column. The column was washed with 1X TE and $dH_2O$ and then the DNA was eluted with 2.5 mL of 50% methanol/50% $dH_2O$. The radioactive DNA elutions were aliquoted into Eppendorf tubes and dried in the speedvac. Once dry, the amount of radioactivity present in each eppendorf tube was determined using a beta scintillation counter.

2.11 Determination of AMM1 and AMM2 DNA molar absorptivities using a UV-Visible Spectrophotometer

The absorption at 260 nm, the absorption maximum for DNA, was determined for AMM1 and AMM2. The absorption was multiplied by the degree of dilution; and for this case, it was 100. The DNA concentration was calculated

using Beer's Law, $A = \varepsilon lc$, where $l = 1$ cm. The molar absorptivities for AMM1 and AMM2 were 205,200 $molar_{-1}$ $cm_{-1}$ and 187,100 $molar_{-1}$ $cm_{-1}$, respectively.

## 2.12 T4 DNA Polymerase Reaction

The T4 DNA polymerase reactions were prepared according to the mixture in Table 2.5. The DNA used in this experiment was single-stranded AMM1 and AMM1 TT. The T4 polymerase was added last to each reaction mixture. The reactions were run for 0, 1, 2, 5, and 10 min at 37 ˚C. The reactions were stopped with 200 $\mu$L hydrazine stop solution and 100% EtOH was added to the reactions. The reactions were ethanol precipitated on dry ice for approximately 1 hr. The samples were examined on an 18% polyacrylamide gel.

## 2.13 Maxam-Gilbert Reactions for Single-Stranded DNA

The reaction mixture consisted of 1X TE, 8 $\mu$M Calf Thymus (CT) DNA, water, and the radioactively labeled single-strand DNA. When fully mixed, the reaction mixture was divided into aliquots of 20 $\mu$L, which had approximately 100,000-200,000 CPM in each sample. The samples were preincubated at the reaction temperature for 5 min each. "No reaction" samples for each radioactive DNA strand were used as controls. For the controls, only hydrazine stop solution and ethanol were added to the 20 $\mu$L aliquots. The Maxam-Gilbert purine reactions (G+A) were reacted at various temperatures and times with 2 $\mu$L piperidine formidate (Table 2.6).

Table 2.5 – T4 DNA Polymerase Reaction

| Material | Amount ($\mu$L) |
|---|---|
| Calf Thymus DNA | 1 |
| 100X BSA | 0.5 |
| 10X NeBuffer2 | 5 |
| T4 DNA polymerase | 1 |
| $dH_2O$ | 42.5 |
| DNA | 2 |

Table 2.5 – Calf Thymus DNA was a DNA carrier used for precipitation purposes. The DNA added in these reactions included AMM1 and AMM1 TT.

Table 2.6 – Piperidine Formidate

| Material | Amount ($\mu$L) |
|---|---|
| Formic Acid | 75 |
| Piperidine | 5 |
| $dH_2O$ | 20 |

Table 2.6 – Add the piperidine last in the solution. Prepare this solution under a hood because when the acid and base are added together the solution smokes. Tap solution gently until mixed and smoking stops.

The Maxam-Gilbert pyrimidine reactions (C+T) were reacted at various temperatures and times with 30 $\mu$L hydrazine. All reactions were stopped by adding 240 $\mu$L hydrazine stop solution for G+A reactions and 200 $\mu$L for C+T reactions. The reactions and stop solution were mixed for 2 minutes, ethanol precipitated on dry ice for 1 hour, and then piperidine treated.

2.14 Maxam-Gilbert G+A Reaction for Double-Stranded DNA

Maxam-Gilbert reagent can react with single-stranded as well as double-stranded DNA. For the double-stranded reactions, AMM1 and its complementary strand AMM2 were annealed prior to the probe reaction. The annealed reaction mixture consisted of 10X TE, which was diluted to 1X TE in the reaction mixture, 8 $\mu$M AMM1, 8 $\mu$M AMM2, $dH_2O$, and the radioactive DNA strand of interest. According to the number of reaction samples, $^{32}$P-labeled DNA was added to acquire between 100,00 CPM to 200,000 CPM per reaction sample. Aliquots of the reaction mixture (20 $\mu$L) were preincubated at temperatures ranging from 0 ˚C to 37 ˚C for 5 min. Then 2 $\mu$L of piperidine formidate was added to each reaction sample and reacted between 2 min and 30 min. "No reaction" control samples were aliquots of the reaction mixtures and only hydrazine stop solution and ethanol were added to them for precipitation purposes. All reactions were stopped by the addition of 240 $\mu$L hydrazine stop solution. The reactions and stop solution were mixed for 2 minutes before ethanol precipitating on dry ice for 1 hour, and then the samples were piperidine treated.

2.15 Maxam-Gilbert C+T Reaction for Double-Stranded DNA

Using the annealed reaction mixture, as described above for the G+A double-stranded reaction, the reaction samples were dispensed in aliquots of 20 $\mu$L each and preincubated at 5 min at various temperatures. The DNA mixtures were reacted with 30 $\mu$L hydrazine for the desired times and temperatures. The no reaction samples for the G+A reaction were used as controls for the C+T reactions because they had the same composition. All reactions were stopped with 200 $\mu$L hydrazine stop solution. The reaction was mixed with the stop solution for 2 minutes and then ethanol precipitated on dry ice for 1 hour and piperidine treated.

2.16 DMS Reaction

This reaction modified guanines in AMM1, AMM2, and AMM1 TT. The reaction mixture consisted of 2X DMS buffer (Table 2.7), which was diluted to 0.2X DMS buffer, 8 $\mu$M AMM1, 8 $\mu$M AMM2, $dH_2O$, and the radioactively labeled DNA of interest. The reaction mixture was distributed into 20 $\mu$L aliquots, which were chilled at 0 ˚C (wet ice) for 5 min prior to reaction. Then 5 $\mu$L of 2.5% DMS (5 $\mu$L DMS in 195 $\mu$L $dH_2O$) was added to each aliquot. AMM1 and AMM1 TT were reacted at 0 ˚C, 25 ˚C, and 37 ˚C for 1 min, 2 min, and 5 min. Then 20 $\mu$L of DMS stop solution (Table 2.8) and 120 $\mu$L ethanol was added to the reactions, which were precipitated on dry ice for 1 hour and piperidine treated.

Table 2.7 – 2X DMS Buffer Formula: for 500 mL

| Material | Amount |
|---|---|
| 100 mM sodium cacodylate | 4.28g |
| 20 mM $MgCl_2$ | 0.8132g |
| 2 mM EDTA | 3.2mL |

Table 2.7 - Sodium cacodylate contains arsenic and is toxic.

Table 2.8 – DMS Stop Solution Formula for 500mL

| Material | Amount |
|---|---|
| 1.5 M sodium acetate | 24.609g |
| 1M 2-mercaptoethanol | 14.03mL |
| 100 $\mu$g/mL t-RNA (100mg in 10mL) | 2mL |

Table 2.8 – 2-mercaptaethanol has a pungent odor and when adding this component to the solution, do so in a hood.

2.17 Potassium Permanganate Reaction

The reaction mixture for the potassium permanganate ($KMnO_4$) reactions consisted of 50 mM sodium cacodylate, 2 mM EDTA, 8 $\mu$M AMM1, 8 $\mu$M AMM2, $dH_2O$, and the radioactively labeled DNA strand. The reaction mixture was distributed into 60 $\mu$L aliquots, which were preincubated at 0 ˚C, 25 ˚C, and 37 ˚C for 5 min. Then 1.5 $\mu$L of 62.5% $KMnO_4$ (19.8 g $KMnO_4$ in 500 mL $dH_2O$) was added to each aliquot. AMM1, AMM2, and AMM1 TT were reacted at 0 ˚C, 25 ˚C, and 37 ˚C for 2, 4, and 6 min. Then 300 $\mu$L of DMS stop solution and ethanol were added to each reaction to precipitate in dry ice for 1 hour. The reactions were ethanol precipitated a second time for 1 hr, suspended in 50 $\mu$L $dH_2O$, 25 $\mu$L 7.5 M $NH_4OAc$, and 215 $\mu$L 100% EtOH and piperidine treated.

2.18 Polyacrylamide Gel for Reaction Analysis

The radioactivity of each DNA reaction was counted using a Beckman Coulter LS 6500 Multi-Purpose Scintillation Counter. 1X running dye was added to the DNA reaction samples at 1 $\mu$L per 10,000 CPM. The DNA and dye were vortexed and heated at 90 ˚C heat for 5min and then between 4-5 $\mu$L (40,000-50,000 CPM) were injected into the wells. Prior to injection, the gel was heated at 50W for approximately 1 hour to get the gel adequately hot so the DNA could remain denatured. The gel was run between 3-4 hours.

## 2.19 Gel Electrophoresis Scan and Quantification

The gel was then put into a Phosphorimager box overnight. Then the Phosphorimager plate was scanned using a Molecular Dynamics Phosphorimager. The gel was quantitated in the ImageQuant program. The reactivity percentages of the bases were determined by their relative volumes in relation to the gel lane volumes. The control DNA percentages were subtracted out from percent base reactivity DNA reactions.

# CHAPTER 3 – RESULTS

## 3.1 Formation and Characterization of Oligonucleotide with a Thymine Dimer Lesion

The thymine dimer lesion was synthesized as previously published on a 19-nucleotide strand using 300 nm UV light and acetophenone, a triplet sensitizer (Chinnapen and Sen, 2004). Characterization of AMM1 and AMM1 TT strands and verification of thymine dimer synthesis was determined using multiple techniques that included HPLC purification, electrospray ionization mass spectrometry, cycloreversal test, Maxam-Gilbert sequencing reactions, and T4 DNA polymerase reaction.

## 3.2 HPLC Purification

After the thymine dimer had been synthesized, the products were purified and characterized using reversed phase HPLC purification (Figure 3.1). Figure 1 is an overlay of the pure AMM1 chromatograph (blue) and the AMM1 TT chromatograph (red). Looking at the red plot on the chromatograph, AMM1 TT eluted as the small broad peak (approximately 17.5-19.9 min) directly before the unreacted AMM1 peak, which eluted at 20 min. The AMM1 and AMM1 TT peaks could never be more thoroughly resolved by HPLC purification despite many changes in solvent ratios of acetonitrile to ammonium acetate.

In addition, the AMM1 TT synthesis did not go to completion and always had a mixture of synthesized dimer strand and unreacted AMM1; therefore, the AMM1 TT yield was low. After HPLC purification, the first thymine dimer synthesis synthesized from 0.5 μmol AMM1 resulted in a 7.8% product yield. A second synthesis of AMM1 TT from 1.5 μmol AMM1 produced a 15.6% yield.

### 3.3 Electrospray Ionization Mass Spectrometry

A thymine dimer mutation results in the formation of two bonds with no change in mass. The theoretical mass of AMM1 without the thymine dimer was 5857 g, which matched the mass of AMM1 TT. Both mass spectra graphs showed similar ion fragmentation pattern, which can be seen in Figures 3.2 and 3.3. Since both AMM1 and AMM1 TT samples had the same mass, then the UV reaction did not generate other lesions, which could have happened if the DNA sample had not been purged of oxygen. If oxygen radicals had reacted with AMM1 during the formation of AMM1 TT, then the spectra would have produced a different mass and ion fragmentation pattern.

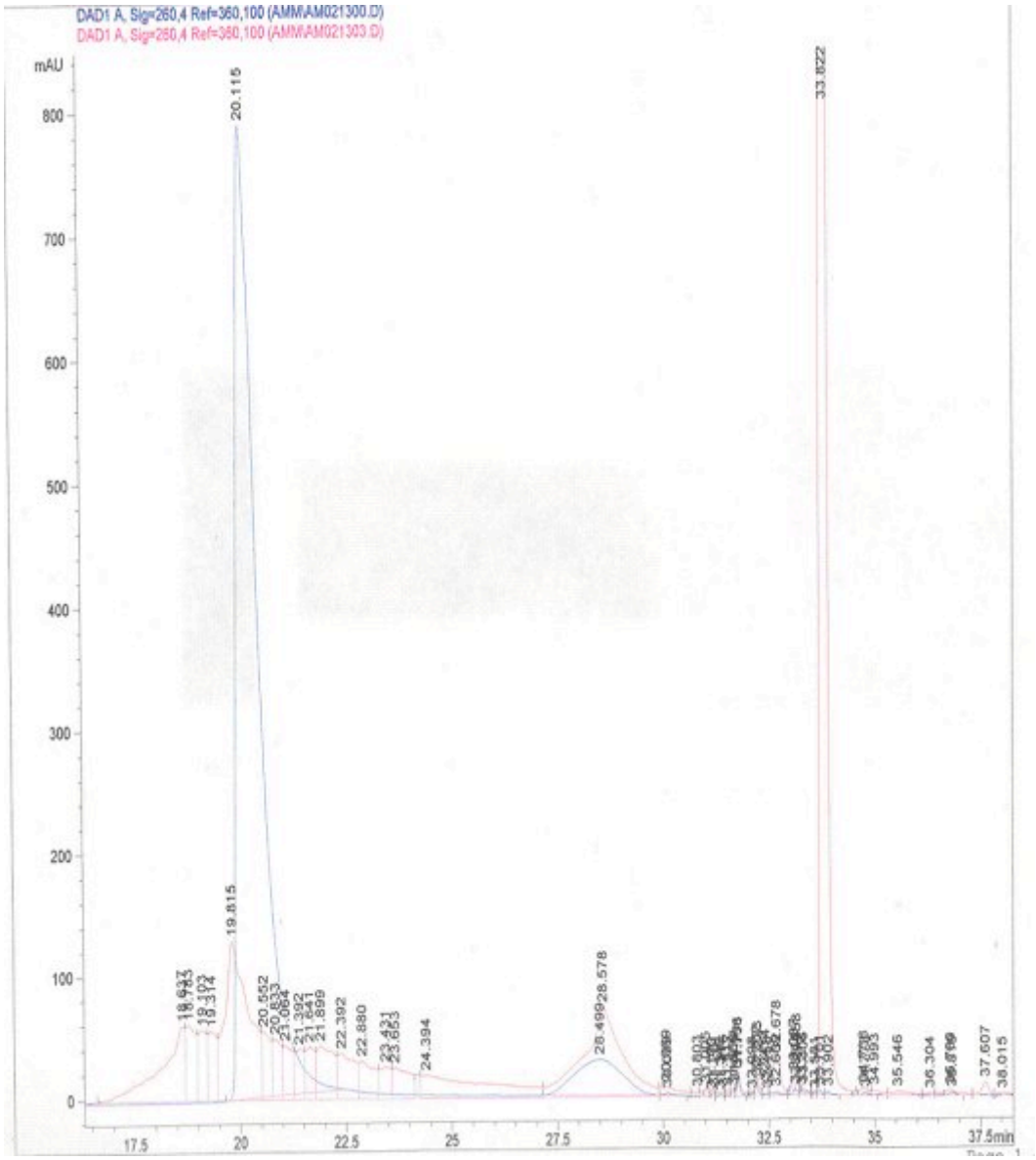


Figure 3.1 – *Overlay of AMM1 and AMM1 TT Chromatographs*: one with pure AMM1 (blue), one with AMM1 TT (red). AMM1 TT was created by reacting AMM1 with UV light and acetophenone. The thymine dimer product can be seen as the new red peak at approximately 18.5 min before the unreacted AMM1 DNA peak at 19.8 min. Acetophenone eluted at 33.8 min. Other damaged products eluted after 20 min.

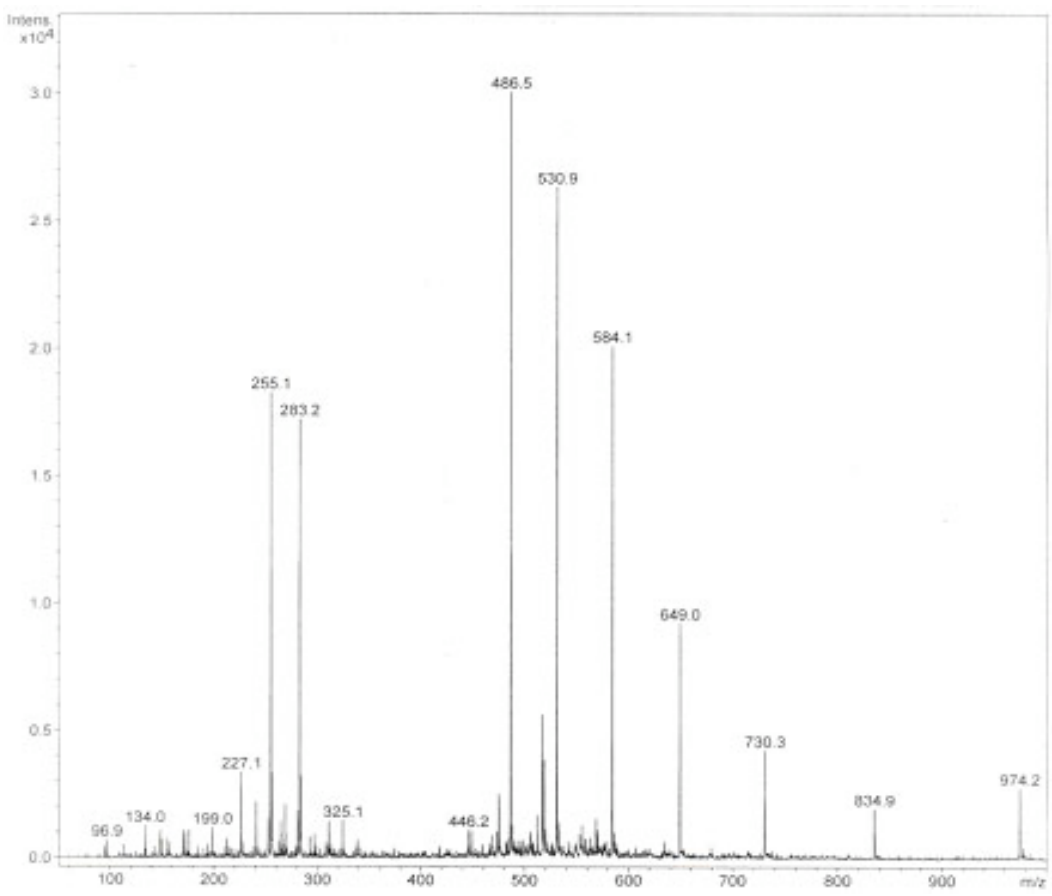


Figure 3.2 – *Mass Spectra of Unmodified AMM1*: The type of mass spectrophotometer used in this experiment was an ESI mass spectrometer. This mass spectra shows the m/z ratio on the x-axis and the peak intensity on the y-axis. The mass spectra of unreacted AMM1 had much less noise than the AMM1 with the dimer because of different concentrations and loading.

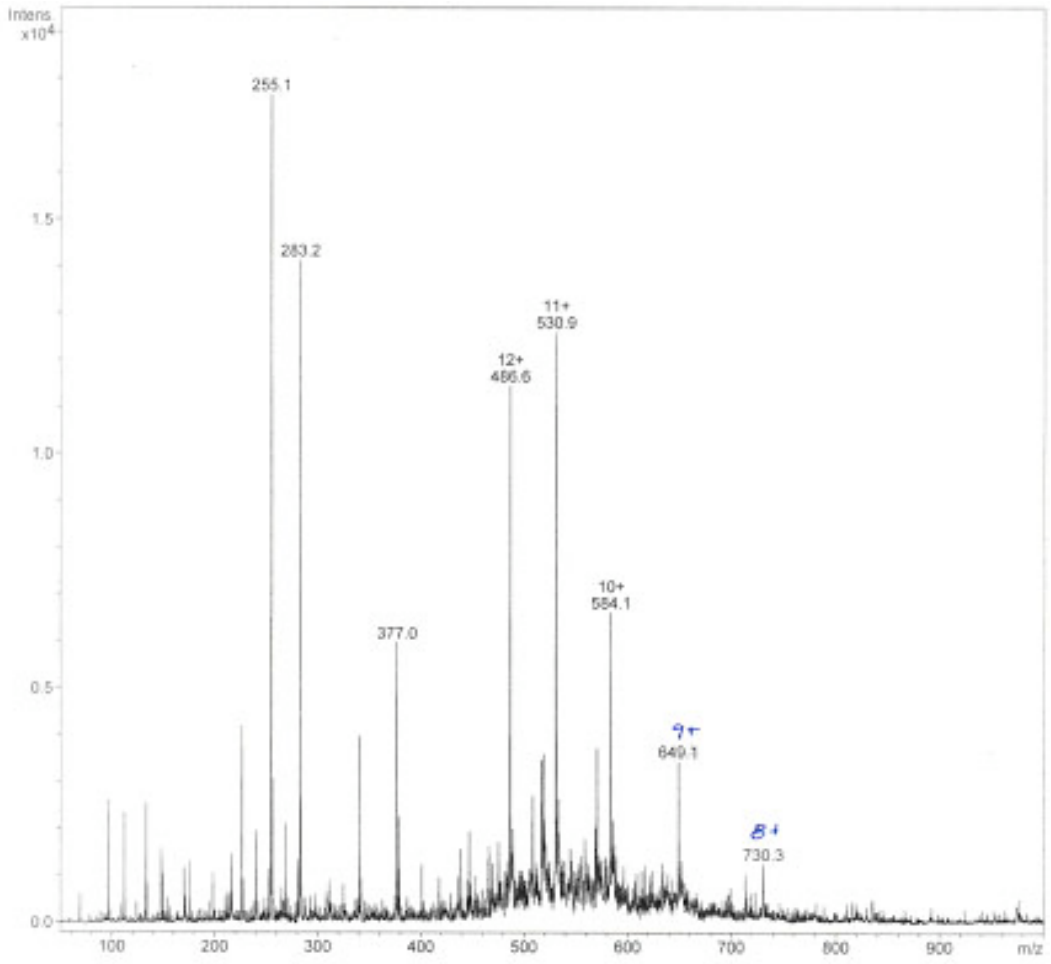


Figure 3.3– *Mass Spectra of AMM1 TT:* The type of mass spectrophotometer used in this experiment was an ESI mass spectrometer. This mass spectra shows the m/z ratio on the x-axis and the peak intensity on the y-axis

### 3.4 Cycloreversal Test

Mass spectrometry determined that both AMM1 and AMM1 TT sequences had the same mass; however, it did not prove the presence of the thymine dimer, merely the absence of other lesion products. Equal masses could indicate that AMM1 TT did not even react to form the thymine dimer. Therefore, a cycloreversal test was done. "Cycloreversal" describes using UV light to convert AMM1 TT back into its unmodified sequence, AMM1, which is in equilibrium with AMM1 TT. Using HPLC analysis, the cycloreversal products produced a chromatograph in which the AMM1 peak grew in intensity and the AMM1 TT peak decreased in intensity (Figure 3.4). Purified AMM1 TT eluted at 18.48 min and purified AMM1 eluted at 19.39 min. The cycloreversal test of pure AMM1 TT resulted in the loss of the AMM1 TT 18.48 min peak, which can be seen as small hump before the cycloreverted AMM1 peak at 19.36 min.

### 3.5 T4 DNA Polymerase

To further confirm the presence of the thymine dimer, the AMM1 TT sequence was reacted with T4 DNA polymerase, which has 3' to 5' exonuclease activity. T4 DNA polymerase cuts DNA at every base in the direction of 3' to 5', but when it encounters a thymine dimer mutation, the enzyme activity terminates at the mutation and can no longer cleave the DNA sequence. With all the DNA strands sequenced on the T4 DNA polymerase gel, seen in Figure 3.5, the exact location of the thymine dimer was determined, which can be seen at thymine 1.

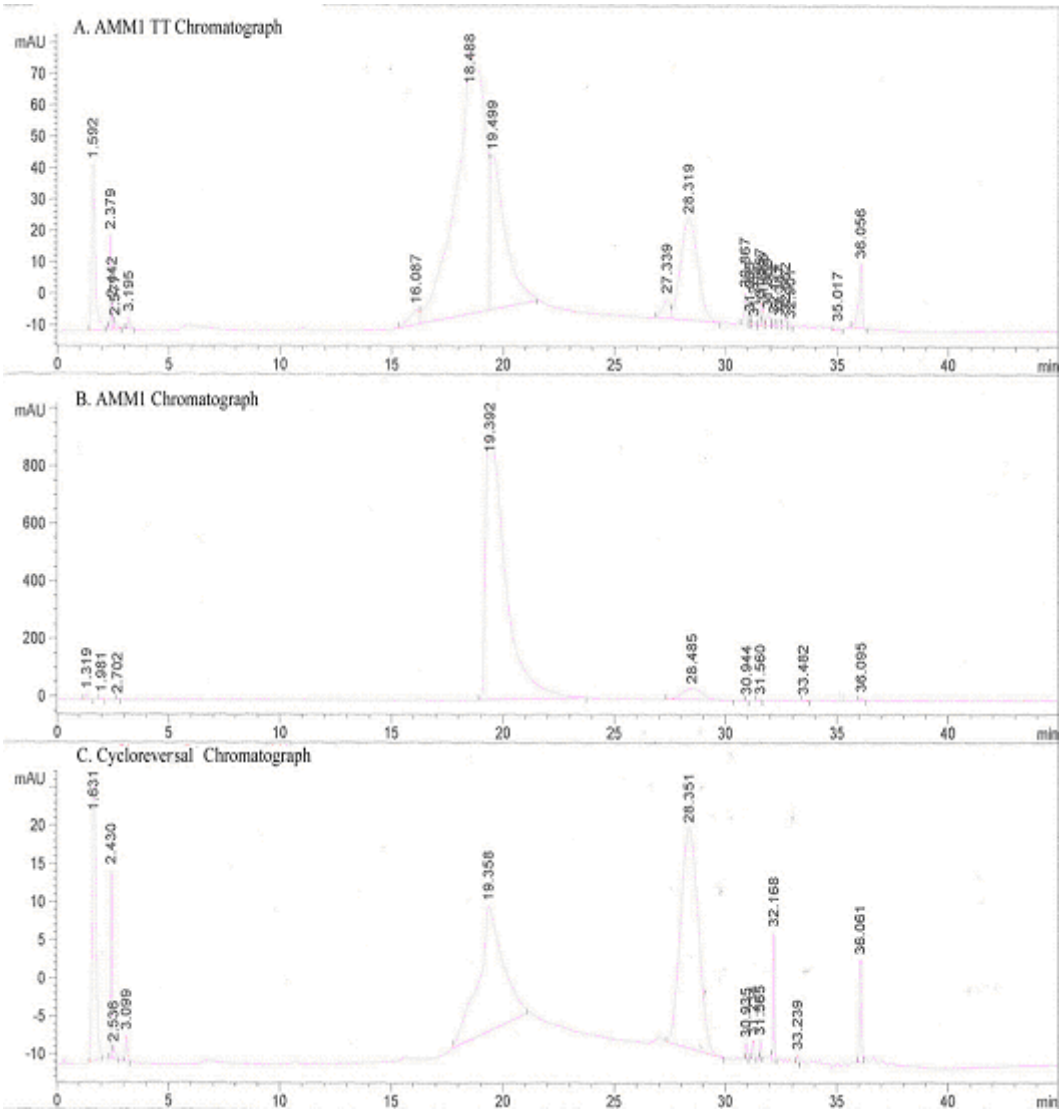


Figure 3.4 – *Cycloreversal Test HPLC Chromatographs:* (A) Purified AMM1 TT elutes at 18.48 min. (B) Purified AMM1 elutes at 19.39 min. (C) The cycloreversal test of AMM1 TT loses its peak at 18.48 min and gains an AMM1 peak at 19.36 min.

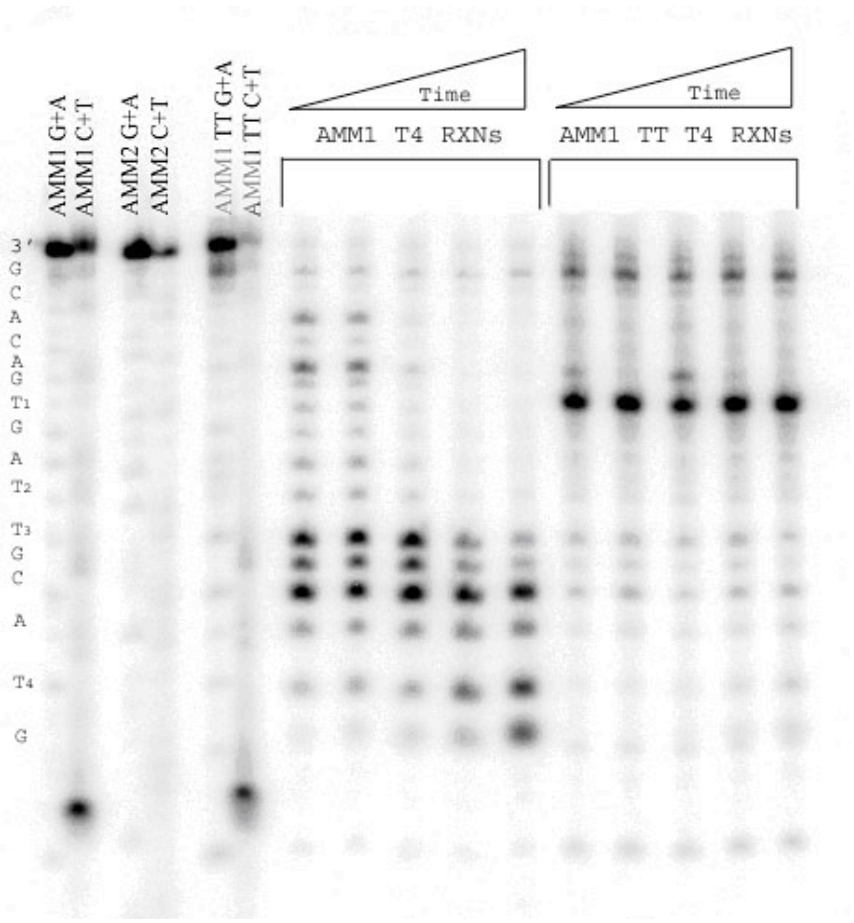


Figure 3.5– *Maxam-Gilbert G+A and C+T Single Strand Sequencing Reactions and T4 DNA Polymerase of AMM1 and AMM1TT from 0-10 min*: AMM1, AMM1 TT, and AMM2 were sequenced as single strands using Maxam-Gilbert G+A and C+T reactions. The other half of the gel is AMM1 and AMM1 TT reacted with the enzyme, T4 DNA polymerase. The time wedges indicate increasing time for AMM1 and AMM1 TT T4 DNA polymerase reactions from first lane at 0 min increasing to 10 min. Only for the AMM1 TT, the T4 DNA polymerase stopped cleaving the DNA before the thymine dimer (T2 and T3); thus, proving the synthesis of the thymine dimer.

The T4 DNA polymerase was incubated with single-stranded oligonucleotides, AMM1 and AMM1 TT, at 0, 1, 2, 5, and 10 minutes to see the progression of reactivity in the exonuclease activity. The AMM1 sequence was cleaved at all of its bases, with base cleavage intensity increasing with time and the size of the remaining pieces of DNA decreasing with time. The cleavage of all the bases in AMM1 signified that the AMM1 sequence did not contain any mutations, which was expected. In the AMM 1 TT sequence, T4 DNA polymerase terminated cleavage of the sequence for every time point at T1, which is located three bases from the thymine dimer towards the 3' end. The termination of the T4 DNA polymerase exonuclease activity at thymine 1 indicated that the thymine dimer lesion had been synthesized.

### 3.6 Probing of Base Accessibility with Small Organic Molecules

Chemical probes were used to examine the thymine dimer mutation site and the bases around the mutation. The specific DNA base reactions that were used to probe the DNA strands included Maxam-Gilbert sequencing reactions for purines and pyrimidines, dimethyl sulfate (DMS), and potassium permanganate ($KMnO_4$). These chemical probes examined the relative base reactivity of AMM1 versus AMM1 TT strands and the complementary strand AMM2 duplexed with AMM1 and AMM1 TT. The data that I was looking for was quantitative proof that the AMM1 TT strand is more reactive than the AMM1 strand with reactivity increasing with time and temperature. Also, I probed to see reactivity differences

between the AMM1 TT mutant strands versus the unmutated AMM1 strand in accordance to structural differences in single-stranded versus double-stranded forms. In addition, the complementary strand (AMM2) of AMM1 and AMM1 TT was examined using DMS and $KMnO_4$ to determine if the presence of a thymine dimer mutation affects the base reactivity of the complementary strand.

### 3.7 Maxam-Gilbert Purine (G+A) reaction

Using conventional DNA sequencing to probe DNA was the first step in examining base reactivity differences between AMM1 and AMM1 TT. The Maxam-Gilbert G+A reaction uses piperidine formidate to create abasic sites at adenine and guanine bases. The reaction was carried out at various temperatures (0 °C, 25 °C, 37 °C) and times (2, 5, 10 min) (Figure 3.6). When visually comparing the gel bands between AMM1 and AMM1 TT, the first thymine from the 3' end of AMM1 TT ran slightly slower than the same thymine in the AMM1 reactions. At initial inspection, the AMM1 Maxam-Gilbert G+A reactions seemed to have greater intensity than the AMM1 TT gel bands, which would indicate overall greater base reactivity for AMM1.

However, this visual assumption was proven false when the quantitated band intensity was subtracted from the background control bands to determine the percent base reactivity of each reacted guanine and adenine base (Figure 3.7). For this reaction, in general, the guanines did not have much reactivity towards piperidine formidate with the percent base reactivities ranging approximately

between –1% and 1.5%. The presence of negative values was due to the subtraction of the control base reactivities (No RXN lanes) from the reaction base reactivities and clearly reflected experimental error of the same magnitude as our base intensity, which is potentially a big problem.

When examining the first guanine graph (G1) of the Maxam-Gilbert G+A reactions, the AMM1 TT strand is slightly more reactive than the AMM1 strand for every temperature. However, at each temperature AMM1 TT reactivity shows a more significant percent G1 reactivity increase, with approximately a 1.5% reactivity increase for each temperature. The correlation between G1 base reactivity and time of reaction was less than 1% increase in reactivity for each time point at 2 min, 5 min, and 10 min.

For the rest of the guanines, G2-G4, there was no clear overall preference in base reactivity between AMM1 and AMM1TT, which were all overlaid on graphs for %G2-G4 reactivity. However, like G1, when examining each temperature, AMM1 TT reactivity had greater guanine reactivity than AMM1, but only at their respective temperatures. Guanines G2-G4 showed an almost indistinguishable increase in reactivity over time for most of the guanine reactions. The reactions at 37 °C for guanines G2-G4 were the only reactions that showed an increase in base reactivity over time. When examining the averaged guanine reactivity, all of the guanines had large error bars according the graphed data. However, the average guanine reactivity was in the range of 1-3% cleaved strands, which is a small percentage.

Adenine 1, which can be seen in Figure 3.8, had similar trends to G1. The AMM1 TT strand reactions were more reactive than the AMM1 strand for every temperature, but the difference in reactivity between AMM1 TT and AMM1 reactions was less than 1%. Similar to G1, at each temperature AMM1 TT reactivity was more significant in percent G1 reactivity increase, with a 0.5% reactivity increase for each temperature. For A1, all of the AMM1 reactions increase with time, but AMM1 TT 37 ºC decreases with time; however since the percent base reactivities are averages, more gels could mitigate this deviation in base reactivity.

For all of the adenines when compared in aggregate, all of the percent base reactivities in the both the AMM1 and AMM1 TT sequences were within the range between 0 to 1% average base reactivity. As for general trends in adenine base reactivity, AMM1 TT adenines were only greater base reactivity than AMM1 adenines for each temperature. As a whole, there was no consensus if adenine reactivity increases with time. The error bars, as with the guanines, were large for the adenine reactivities, with some at a 2% standard deviation. However, since the average base reactivity was so low, the error bars were disproportionately large and if the reactivity could have increased, then the error bars would not have been so large.

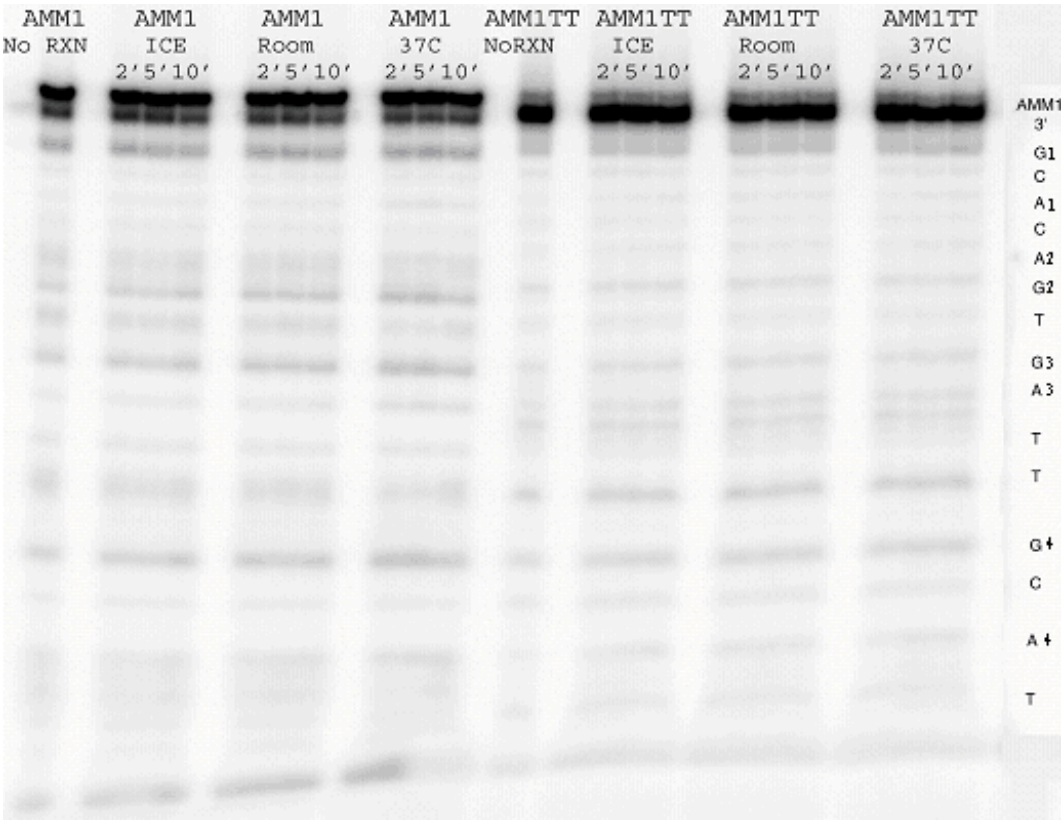


Figure 3.6 – *Maxam-Gilbert Purine (G+A) Reactions of Double-Stranded AMM1 and AMM1 TT Separated on a Polyacrylamide Gel*: This gel represents the guanine and adenine bases of AMM1 and AMM1 TT that were reacted with piperidine formidate. The No RXN lanes were the controls the AMM1 and AMM1 TT reactions. The base reactivities of the No RXN lanes were subtracted out when determining the base reactivities for the reactions. Double-stranded AMM1 and AMM1 TT were reacted for 2 min, 5 min, and 10 min at each of the following temperatures: 0 ºC, 25 ºC, and 37 ºC. Each spot, i.e. reacted base, can be matched up to the DNA sequence located on the right of the gel.

Figure 3.7 – *Average Guanine Reactivity of Double-Stranded AMM1 and AMM1TT for Maxam-Gilbert G+A Reactions*: This graph represents the % guanine reactivity of double-stranded AMM1 and AMM1 TT reacted with piperidine formidate at 0 ºC, 25 ºC, and 37 ºC for 2 min, 5 min, and 10 min. The AMM1 reactions are indicated in red and AMM1 TT reactions are in blue. The reactions at 0 ºC are indicated by squares, 25 ºC reactions are circles, and 37 ºC reactions are triangles. The data points and error bars for this graph and the following graphs for G1-G4 are averages of three Maxam-Gilbert G+A polyacrylamide gels.

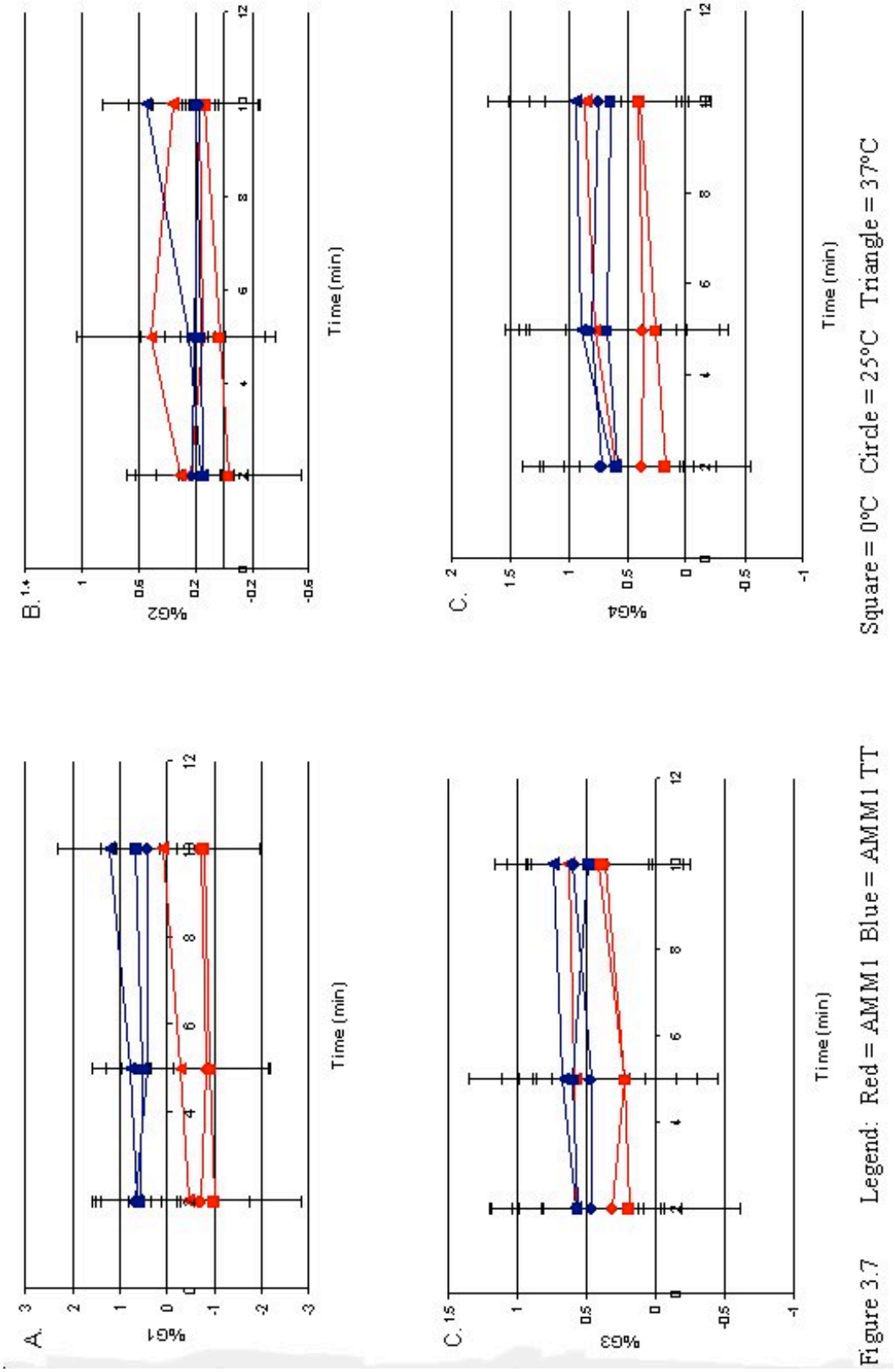


Figure 3.7 Legend: Red = AMM1 Blue = AMM1 TT Square = 0°C Circle = 25°C Triangle = 37°C

Figure 3.8 – *Average Adenine Reactivity of Double-Stranded AMM1 and AMM1TT for Maxam-Gilbert G+A Reactions*: This graph represents the % adenine reactivity of double-stranded AMM1 and AMM1 TT reacted with piperidine formidate at 0 ºC, 25 ºC, and 37 ºC for 2 min, 5 min, and 10 min. The AMM1 reactions are indicated in red and AMM1 TT reactions are in blue. The reactions at 0 ºC are indicated by squares, 25 ºC reactions are circles, and 37 ºC reactions are triangles. The data points and error bars for this graph and the following graphs for A1-A4 are averages of three Maxam-Gilbert G+A polyacrylamide gels.

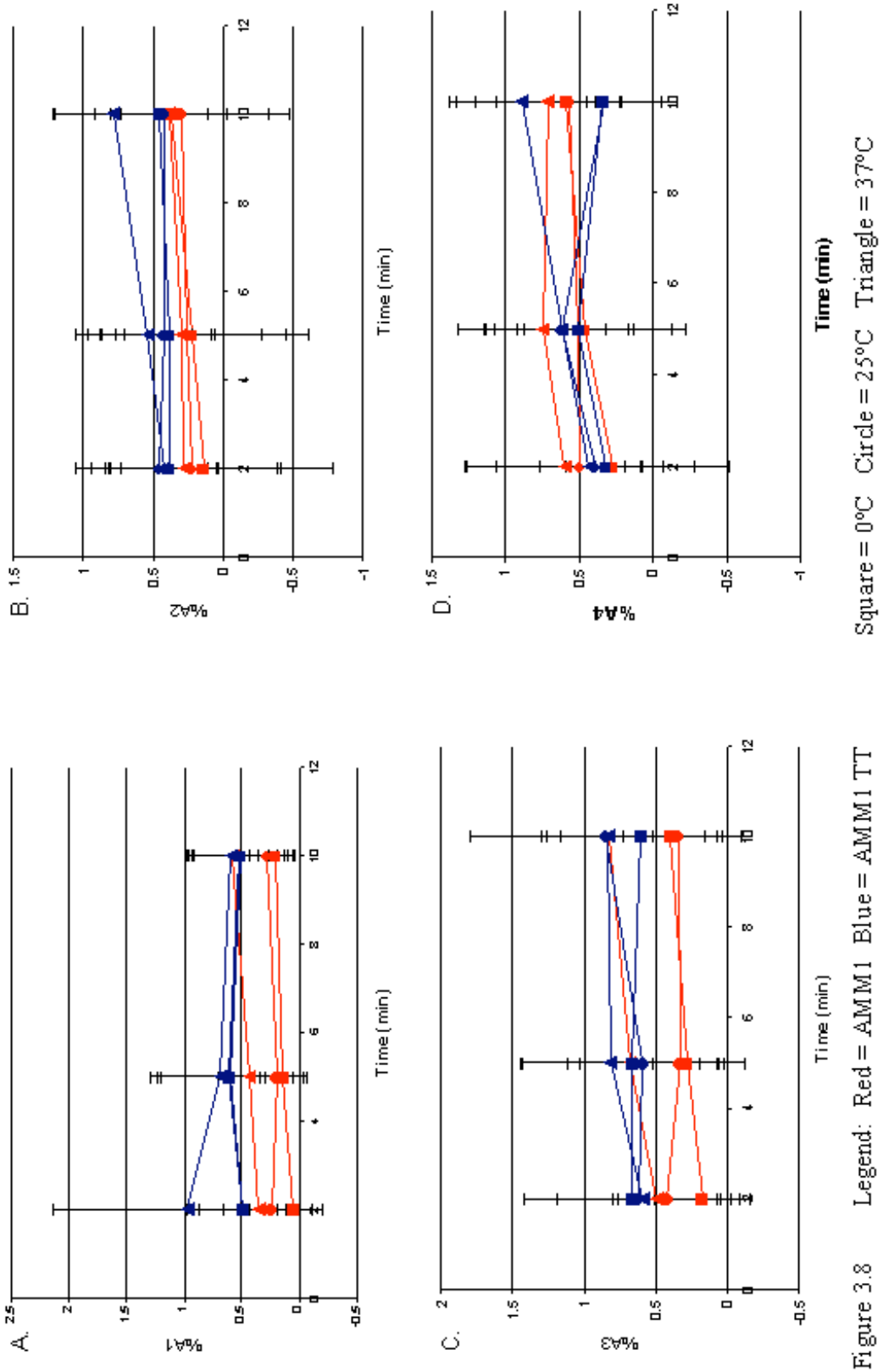


Figure 3.8 Legend: Red = AMM1 Blue = AMM1 TT Square = 0°C Circle = 25°C Triangle = 37°C

3.7A – Maxam-Gilbert Purine Reaction – New Reagent

To increase the signal relative to the noise of the percent base reactivity, reagent reactivity with DNA was assessed and improved upon. Several ratios of formic acid to piperidine reagents were reacted with AMM1 at 37 ºC for 30 min. The pH values of the reagents can be seen in Table 3.1. The reagent that reacted best with duplex AMM1 was 10% formic acid with no piperidine. 10% formic acid produced the most intense purine bands on the gel (Figure 3.9).

Using 10% formic acid, single-stranded and double-stranded AMM1 were reacted with the new reagent at 37 °C for 10 min, 20 min, and 30 min with some reactions in water and others in 1X TE buffer. In this gel, I was looking for increased overall reactivity with the new reagent. In addition, I wanted to compare single strand reactivity to double strand reactivity to see in the reagent was more reactive towards single-stranded DNA due to base accessibility. The final comparison was two sets of single-stranded reactions and double-stranded reactions with one set using only water and the other in the presence of 1X TE buffer. Reactions in water would be expected to be more reactive because DNA structure is less stable in water and more stable in buffer to shield the charged sugar-phosphate backbone.

When qualitatively examining the gel in Figure 3.10, the purine gel bands are darker than previous Maxam-Gilbert purine reaction gels. However, when the AMM1 reactions and AMM1 TT reactions were visually compared to their "no reaction" controls, the gel bands for the reactions did not seem to be significantly

darker than the controls. This qualitative observation was verified when the quantitated base reactivies of the purine gel bands were investigated. The double and single-stranded AMM1 percent guanine and adenine reactivity seemed to minimally prefer the presence of water instead of buffer (Figure 3.11). The guanine and adenines had the same trends of increasing base reactivity over time and temperature for the water and 1X TE reactions. However, the majority of the purine reactions for this gel have reactions that overlaid so no clear correlation of reactivity preference between single strand versus double strand base reactivity could be made. The new reagent did not produce significantly higher base reactivities for either guanines or adenines. With the exception of G1, which had a maximum of 2.5% G1 reactivity, the other guanines all had base reactivities under 1.2%, and all the adenines had reactivities under 1.3%, which was still not a large enough percent base reactivity to determine probe reactivity preference. Single-stranded reactions were more reactive for guanines, but double-stranded reactions were more reactive for adenines. Therefore, no trend of DNA structural preference could be determined. Previously it was hypothesized that the buffer could have been inhibiting the rate of reaction of the piperidine formidate, but the water reactions were only 0.1% more reactive than the 1XTE reaction. In addition, despite that the reactions were run for a longer time than previous Maxam-Gilbert reaction at 10-30 min, the base reactivity did not increase much from the Maxam-Gilbert G+A reaction seen in the previous gel, which ranged between –1 to 1.2% guanines and 0 to 1% in adenines.

Table 3.1 – New Maxam-Gilbert Reagents

| % Formic Acid | Amount of Piperdine (μL) | pH |
|---|---|---|
| 4% | 0 | 0-1 |
| 4% | 5 | 3 |
| 4% | 10 | 4-5 |
| 4% | 20 | 10-11 |
| 10% | 0 | 0-1 |
| 10% | 10 | 3 |
| 10% | 40 | 4-5 |

Table 3.1 – Varied ratios of formic acid to piperidine to obtain a range of pH values to react with AMM1. pH was determined using litmus paper.

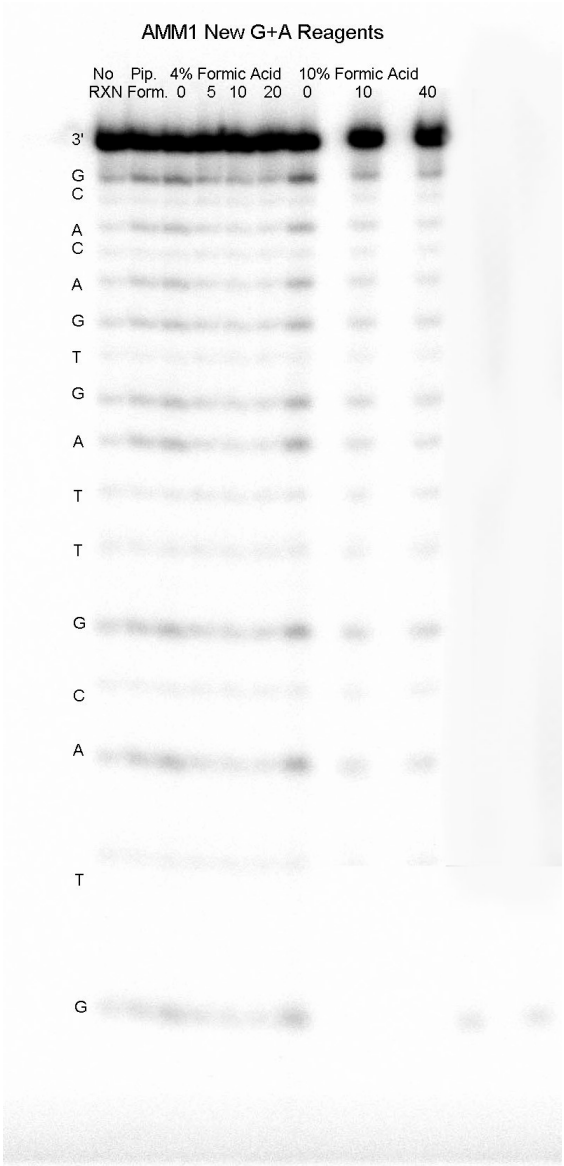


Figure 3.9 – *New Maxam-Gilbert G+A Reagents*: All of the reagents were reacted with AMM1 at 37 ºC for 30 min. The tested reagents are as follows: piperidine formidate (original reagent), 4% formic acid with 0 µL, 5 µL, 10 µL, or 20 µL of piperidine added, and 10% formic acid with 0 µL, 10 µL, or 40 µL of piperidine added. The most reactive reagent was 10% formic acid with 0 µL piperidine.

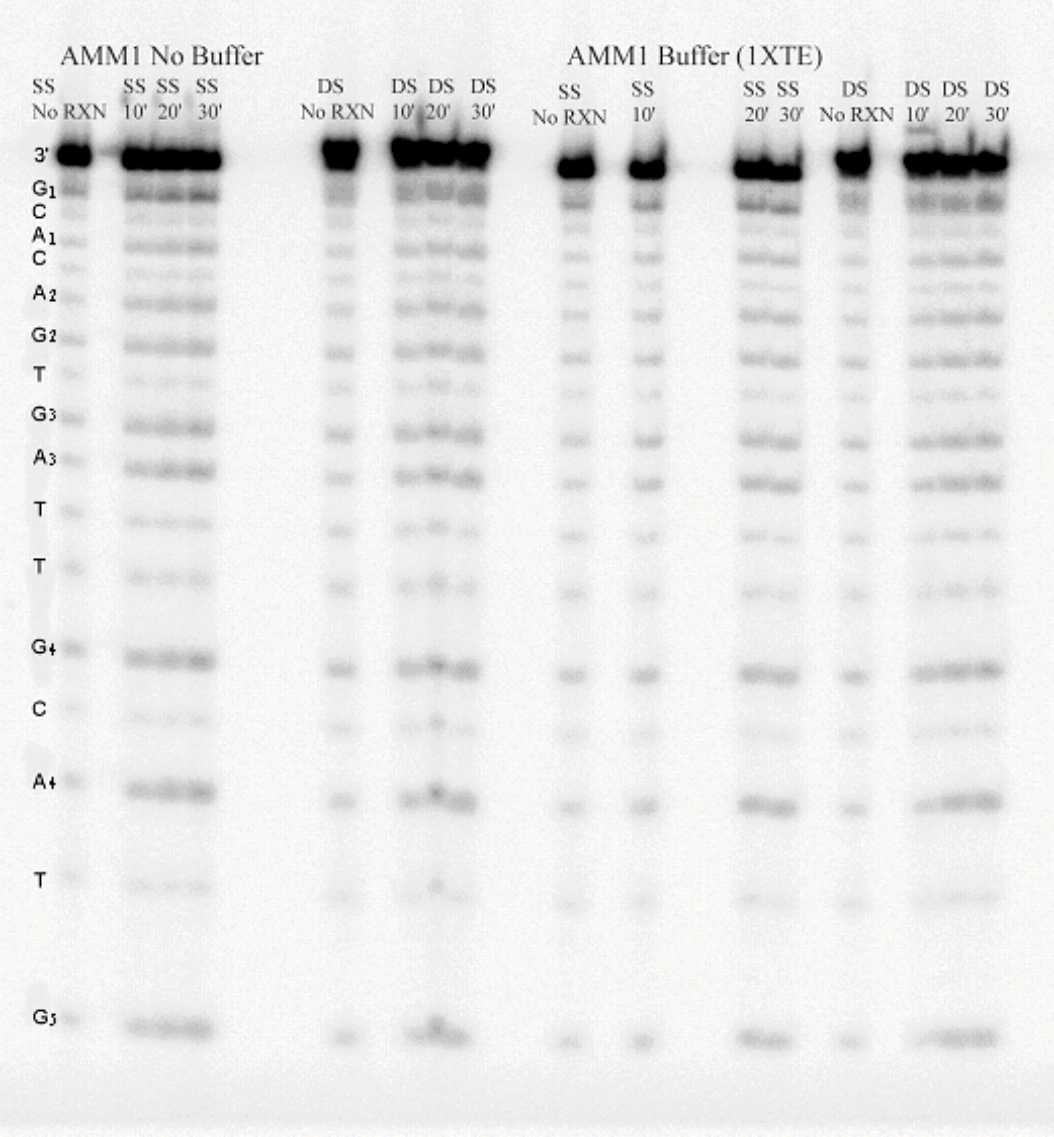


Figure 3.10 – *Single-Stranded and Double-Stranded AMM1 Reacted with the New Reagent:* Single-stranded and double-stranded AMM1 in water and 1X TE were reacted with 10% formic acid, instead of the typical reagent, piperidine formidate, which is a ratio of formic acid to piperidine. The bases can be matched up with the sequence running parallel on the gel.

Figure 3.11 – *%G1 and %A1 Reactivity for Maxam-Gilbert G+A Reactions of Single-Stranded and Double-Stranded AMM1 Reacted with 10% Formic Acid in $H_20$ and 1X TE:* All reactions were carried out at 10, 20 and 30 minutes at 37 ºC. The single-stranded reaction in water is blue. The single-stranded reaction in 1XTE buffer is pink. The double-stranded reaction in water is orange. The double-stranded reaction in 1XTE buffer is green. The %G1 and %A1 are characteristic graphs for guanine and adenine percent base reactivity.

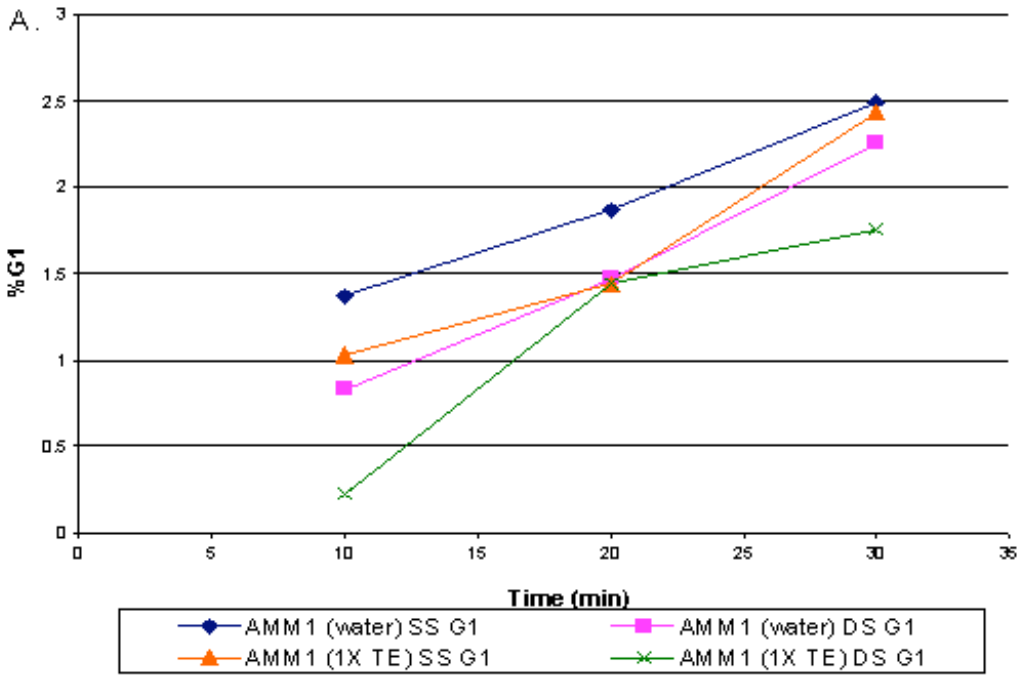
A.
%G1
Time (min)
AMM1 (water) SS G1
AMM1 (water) DS G1
AMM1 (1X TE) SS G1
AMM1 (1X TE) DS G1

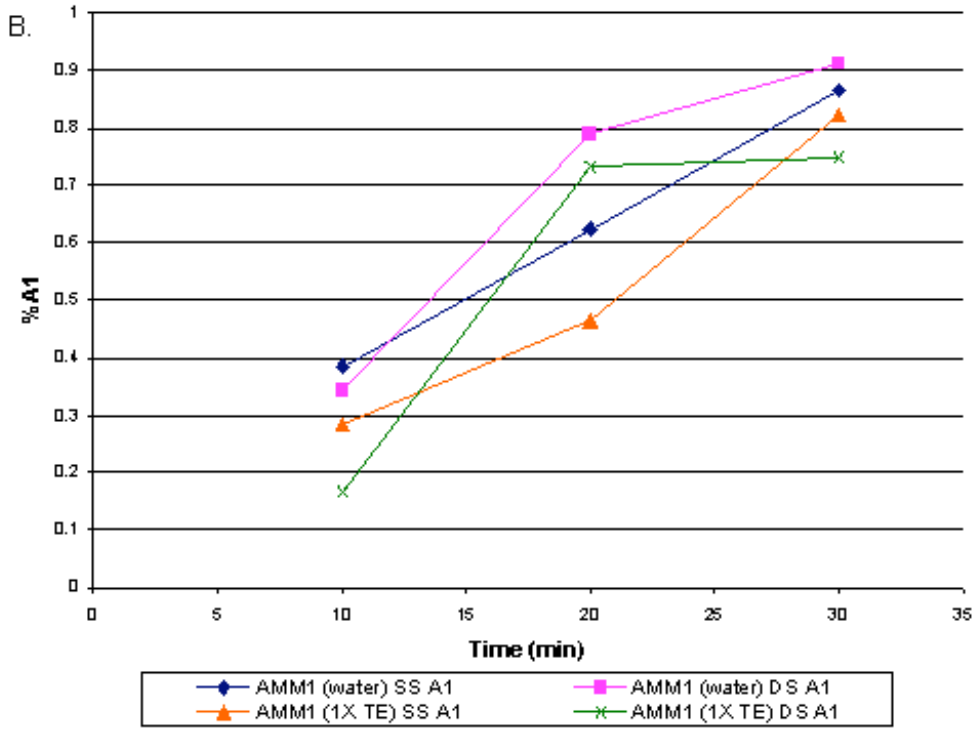
B.
%A1
Time (min)
AMM1 (water) SS A1
AMM1 (water) DS A1
AMM1 (1X TE) SS A1
AMM1 (1X TE) DS A1

Figure 3.11

### 3.8 Maxam-Gilbert Pyrimidine (C+T) Reaction

The reagent used in the pyrimidine reactions was hydrazine base (pH = 14) that attacks at C6 of the pyrimidine, and the addition of piperidine cleaves the DNA strand at the pyrimidine. Like the Maxam-Gilbert G+A reactions, the pyrimidine reactions were not reactive towards double-stranded DNA, even in the presence of a thymine dimer mutation, which can be seen on Figure 3.12. The pyrimidine bands are almost indistinguishable from the background of control reaction (No RXN) gel lanes. Gel bands for AMM1 and AMM1 TT at each incubation temperature had almost the same intensity. In addition, the Maxam-Gilbert C+T reactions frequently produced a gel that was unable to be quantitated accurately due to low intensity blurred gel bands. Hydrazine was therefore not a useful probe for AMM1 and AMM1 TT.

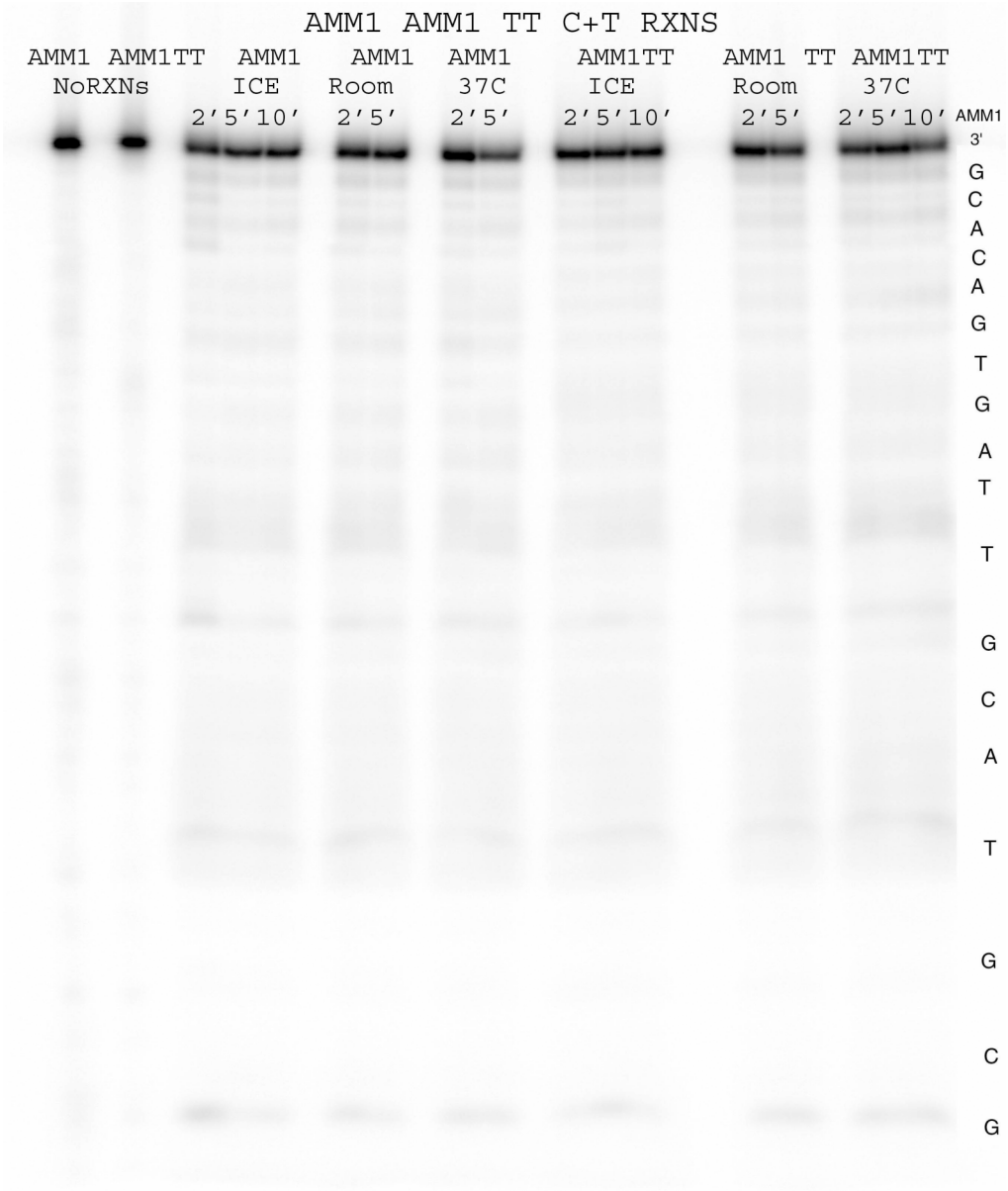


Figure 3.12 – *Maxam-Gilbert Pyrimidine (C+T) Reaction for Double-Stranded AMM1 and AMM1 TT*: Double-Stranded AMM1 and AMM1 TT were reacted with hydrazine at 0 ºC, 25 ºC, and 37 ºC for 2 min, 5 min, and 10 min.

3.9 Dimethyl Sulfate Reaction Quantification

The next step was to examine guanines using dimethyl sulfate (DMS). Both the G+A reaction and DMS react in the major groove. However, DMS reacts by a different pathway, methylating mainly the N7 of guanine. When examining the DMS reaction on a polyacrylamide gel, as the incubation temperatures and time increase, guanine band intensity generally increased (Figure 3.13). The base intensities were strong, well above the background base intensities. Since the signal was stronger, this reaction could report more clearly about base accessibility for AMM1 versus AMM1 TT.

When examining the average percent base reactivity for guanine 1 (G1), this guanine had a range of reactivity between -1 and 3.7% base reactivity for AMM1 and AMM1 TT, which was greater than the Maxam-Gilbert G+A reaction (Figure 3.14). Of the reactions, AMM1 DS 37 ºC was the most reactive sequence for G1; however, most of the AMM1 TT reactions overlaid the AMM1 reactions, so no clear statement could be made that AMM1 is more reactive than AMM1 TT. For each DNA strand, the double-stranded reactions were more reactive than the single-stranded reactions for AMM1 and AMM1 TT for each respective temperature. However, like the Maxam-Gilbert G+A reaction, some of the quantitated base reactivities for G1 reaction of AMM1 TT SS at 25 ºC were negative, which meant that the control reaction were greater in signal intensity than that actual reaction with the DMS reagent.

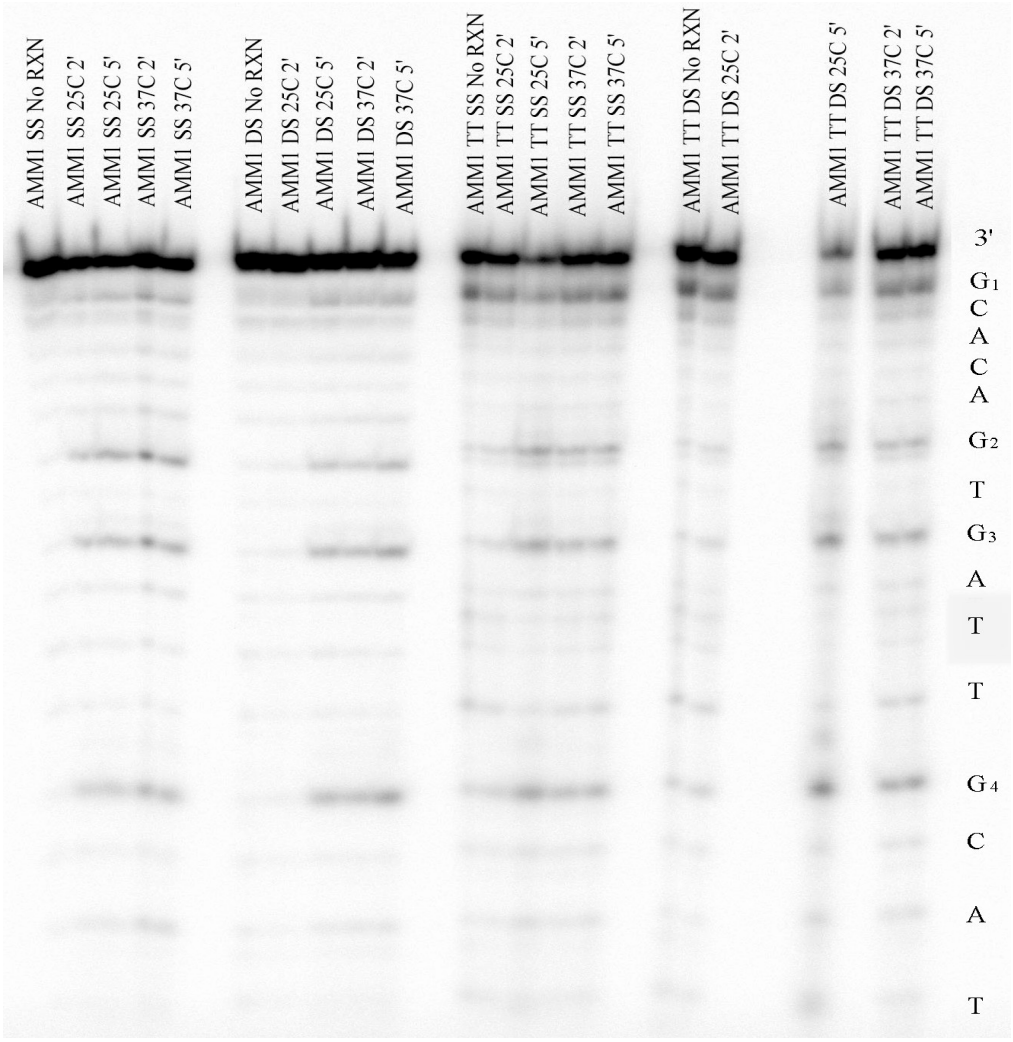


Figure 3.13 – *DMS Reactions: Double-Stranded (DS) and Single-Stranded (SS) AMM1*: These DMS reactions were carried out on single and double-stranded AMM1 and AMM1 TT sequences at 25 ºC and 37 ºC for 2-5 minutes. The No RXN lanes were the controls the AMM1 and AMM1 TT reactions. The reactivity of the No RXN lanes were background and were subtracted out when determining the base reactivities for the reactions. Each reacted base can be matched up to the DNA sequence located on the right of the gel.

Figure 3.14 – *%Guanine Reactivity for Single and Double Strand AMM1 and AMM1 TT*: This graph represents the % guanine reactivity with 2.5% DMS at 25 ºC and 37 ºC for 2 min and 5 min. The AMM1 reactions are indicated in red and AMM1 TT reactions are in blue. The reactions at 25 ºC reactions are circles and 37 ºC reactions are triangles. The data points and error bars for the graphs of %G1 through %G4 are averages of four Maxam-Gilbert DMS polyacrylamide gels.

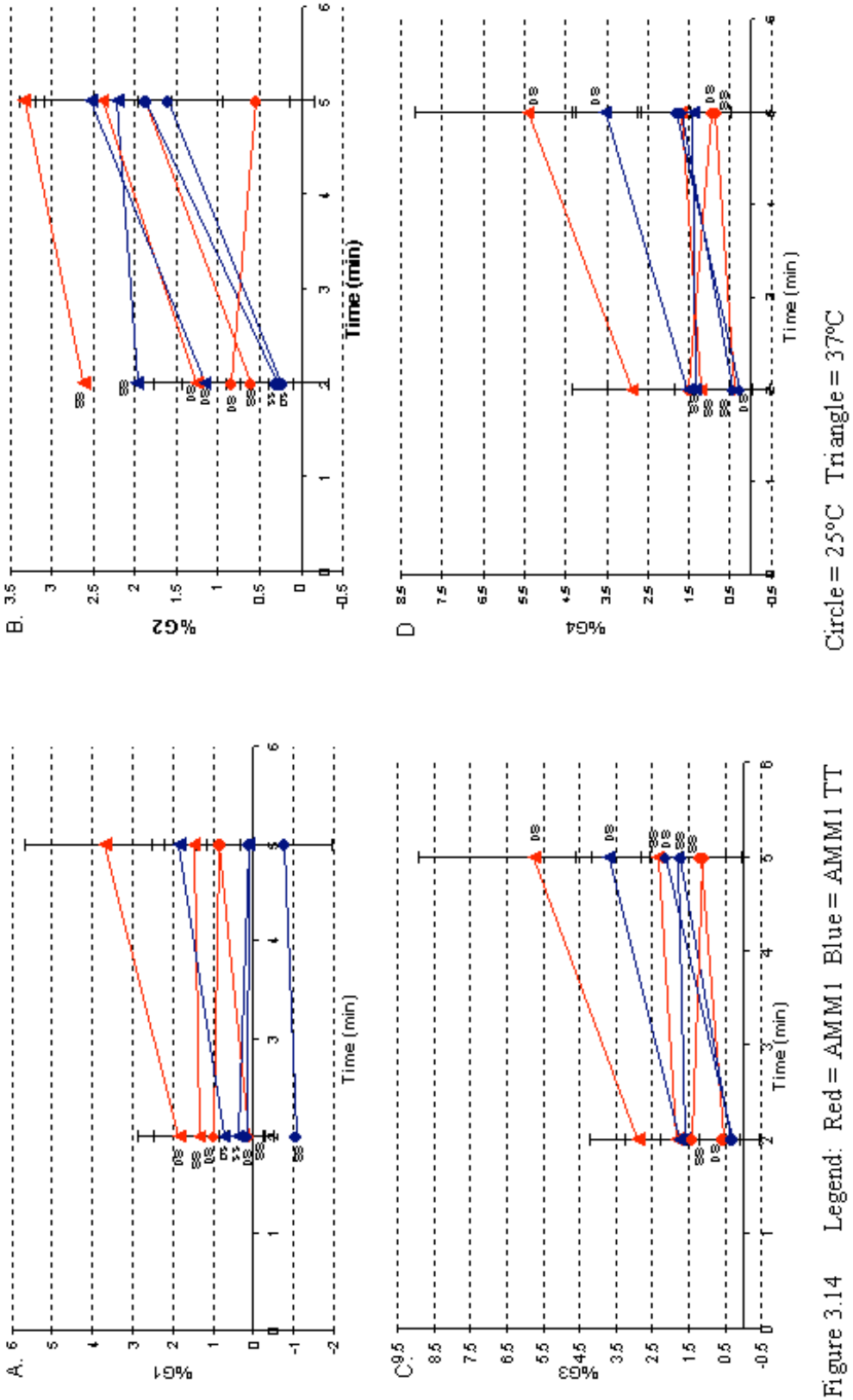


Figure 3.14 Legend: Red = AMM1 Blue = AMM1 TT Circle = 25°C Triangle = 37°C

When examining the guanine reactivity for DMS reactions in aggregate, AMM1 and AMM1 TT guanines generally increased with greater temperature and time, with the exception of a few data points that decreased over time. AMM1 tended to be the more reactive sequence towards DMS, but it was not a consistent trend. For G3 and G4, double-stranded reactions were more reactive that the single-stranded reactions, and for G1 and G2, single-stranded reactions were more reactive that the double-stranded reactions. Most of the percent guanine data points for AMM1 and AMM1 TT had large standard deviations and data points overlaid with each other.

### 3.10 Potassium Permanganate Reaction Results

Potassium Permanganate ($KMnO_4$) oxidizes primarily thymines in DNA. In comparison to the reactions previously discussed, the $KMnO_4$ reaction gave noticeably different patterns of base reactivity for AMM1 versus AMM1 TT (Figure 3.15). The thymines T2 and T3 were less reactive within the thymine dimer, and the other thymines, T1 and T4, were more reactive in the AMM1 TT stand than AMM1.

When qualitatively examining the polyacrylamide gel of a set of single and double-stranded AMM1 and AMM1 TT $KMnO_4$ reactions, the thymines on the AMM1TT DNA sequence reacted very differently from the unmodified AMM1 sequence. AMM1 TT was more reactive at T1 than AMM1. Also, at T2 and T3, which were the thymine bases involved in the AMM1 TT thymine dimer,

AMM1 TT was noticeably less reactive than the same thymines on AMM1. Thymine 4 of AMM1 TT for both single-stranded reactions and double-stranded reactions appeared to have equal gel band intensity to AMM1 reactions in single-stranded form, but more reactive than AMM1 in the double-stranded form. For both AMM1 and AMM1 TT, the thymine bands of their single-stranded reactions appeared to be greater in signal intensity than their double-stranded reactions.

Thymine 1 (T1), which is the thymine closest to the 3' end of the DNA sequence, showed very interesting reactivity trends for the AMM1 and AMM1 TT sequence (Figure 3.16). T1 had preferential $KMnO_4$ reactivity for the AMM1 TT sequence, which had base cleavage reactivity ranging between 3-9%. AMM1 had some reactivity towards $KMnO_4$ at T1, but the percent reactivity was less than 2%. When examining the single strand versus double strand reactions for T1, AMM1 and AMM1 TT single-stranded reactions were more reactive than their corresponding double-stranded reactions at the same times and temperatures.

Thymine 2 (T2) and thymine 3 (T3) had very interesting reactivities because both thymines were involved in the thymine dimer complex in AMM1 TT. For T2 and T3, AMM1 was substantially more reactive than AMM1 TT. The single strand reactions for T2 and T3 were more reactive than the double strand reactions for both AMM1 and AMM1 TT. However, the gaps in reactivity between single and double strand reactions varied greatly for AMM1 versus AMM1 TT. AMM1 TT single strand reactions for 25 ºC and 37 ºC were only

about 1% more reactive than the double strand reactions. However, AMM1 had approximately a 10% increase in reactivity for single strand reactions.

Thymine four (T4) did not have as clear trends as the previously discussed thymine bases. The only clear trend is that the double strand AMM1 reactions were lowest in %T4 reactivity. The rest of the data points overlay so no clear preference for the AMM1 versus AMM1 TT sequence could be made. However, AMM1 and AMM1 TT single-stranded reactions were more reactive than their corresponding double-stranded reactions only at their respective times and temperatures.

### 3.11 AMM2 Reactivity probed with DMS and $KMnO_4$

After thoroughly probing the AMM1 and AMM1 TT sequences, the DMS and $KMnO_4$ reagents were used to examine the complementary strand, called AMM2. The AMM2 strand is complementary to both AMM1 and AMM1 TT. By probing AMM2 duplexed with AMM1 and AMM1TT, information about the bases opposite a thymine dimer or normal unmutated bases could be extrapolated.

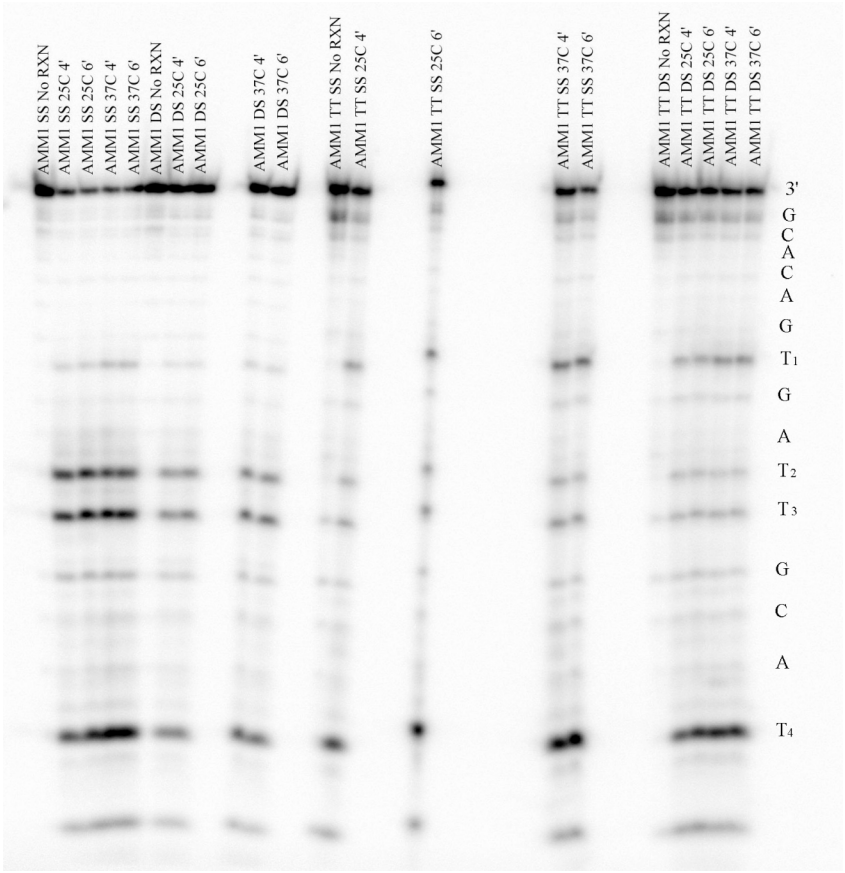


Figure 3.15 – *$KMnO_4$ Reactions: Single and Double-Stranded AMM1 and AMM1TT at 25 ˚C and 37 ˚C for 4-6 min:* This gel represents the thymine bases of AMM1 and AMM1 TT that were reacted with $KMnO_4$. The No RXN lanes were the controls the AMM1 and AMM1 TT reactions. The reactivity of the No RXN lanes are background base reactivity from piperidine cleavage and were subtracted out when determining the thymine reactivities for the reactions. Double-Stranded AMM1 and AMM1 TT were reacted for 4min and 6min at each of the following temperatures: 25 ºC and 37 ºC. Each spot, which represents the base's reactivity towards $KMnO_4$, can be matched up to the DNA sequence located on the right of the gel.

Figure 3.16 – *$KMnO_4$ Reactions: %Thymine reactivity for AMM1 and AMM1TT at 25 ˚C and 37 ˚C for 4-6 min:* These graphs represents the % thymine reactivity of single and double-stranded AMM1 and AMM1 TT reacted with 62.5mM $KMnO_4$ at 25 ºC and 37 ºC for 4 min and 6 min. The AMM1 reactions are indicated in red and AMM1 TT reactions are in blue. The reactions at 25 ºC reactions are circles and 37 ºC reactions are triangles. The data points and error bars for these graphs for T1 through T3 are averages of four $KMnO_4$ polyacrylamide gels. No error bars were made for the SS reactions because there were only two gels with $KMnO_4$ SS reactions. The T4 graph does not have error bars because the data points are only averages of two gels. T4 was difficult to retain on the gels because it is the thymine closest to the 5' end of the DNA sequences.

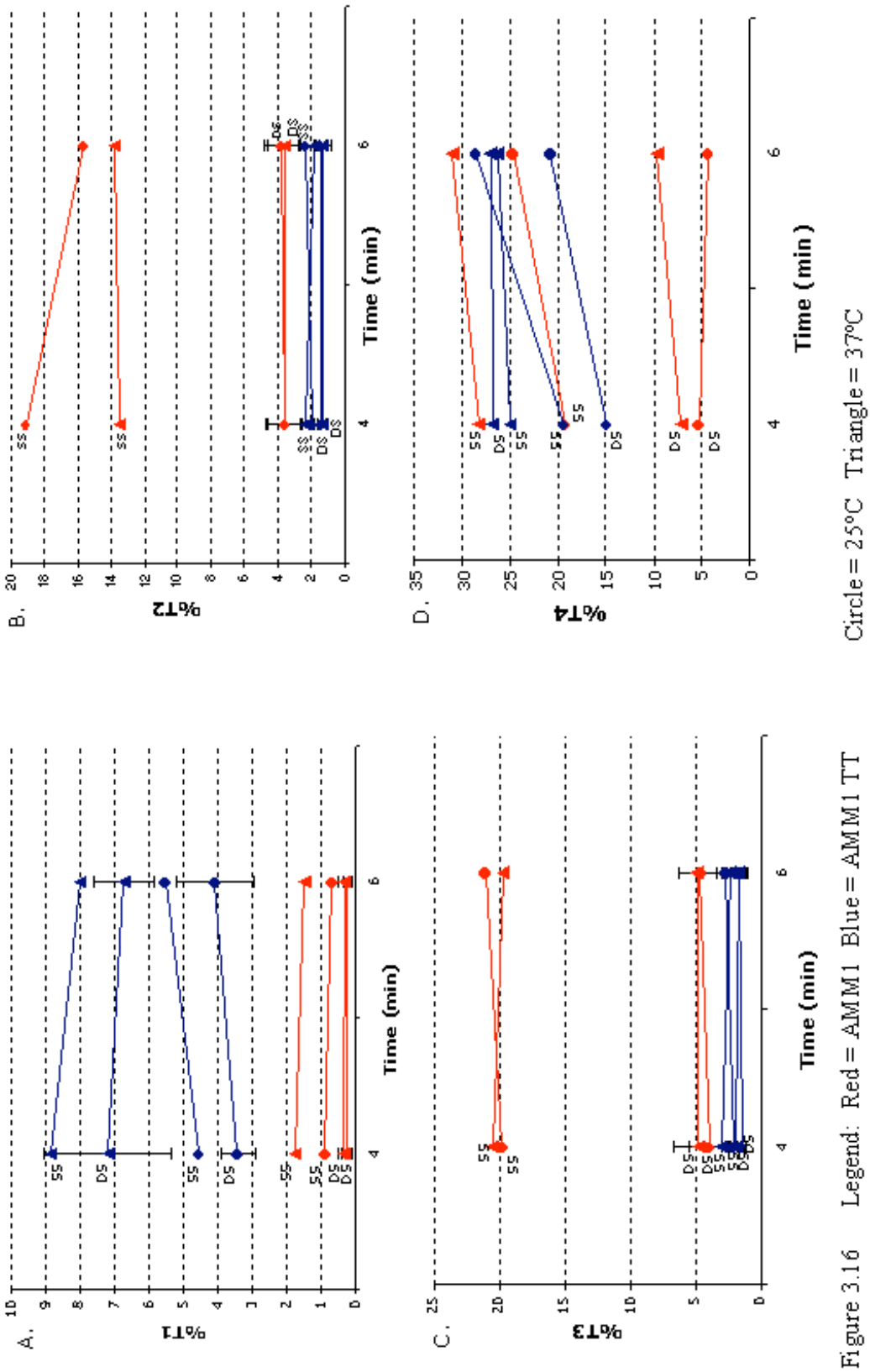


Figure 3.16 Legend: Red = AMM1 Blue = AMM1 TT Circle = 25°C Triangle = 37°C

3.11a. DMS Reactions with AMM2

The AMM2 strand had three guanines that were probed with DMS. The DMS reactions probed AMM2 duplexed to AMM1 and AMM1 TT in a temperature range of 0 ºC to 37 ºC and the reactions were set for the following times: 1 min, 2 min, and 5 min. From a qualitative perspective, when looking at the gel in Figure 3.17, it was obvious that guanines 1-3 had reactivity well above the controls, which were designated as the No RXN lanes.

Guanine reactivity of AMM2 had similar trends to the previous AMM1 and AMM1 TT DMS reactions (Figure 3.18). There was no clear correlation of sequence preference for DMS on the AMM2 sequence duplexed with AMM1 or AMM1 TT. All of the data points for the different sequences and temperature reactions had very similar percent guanine reactivities in comparison to each other and most data points overlaid. For some guanines, reactions at 25 ºC were more reactive than 37 ºC and then vice versa for other guanines. One oddity of this reaction was the AMM2 reaction duplexed with AMM1 TT 25 ºC at 1 min, in which every guanine of that reaction had a large percent reactivity. All guanines for AMM2 duplexes with AMM1 and AMM1 TT had a range of percent base reactivity between 0 and 3%, with the exception of the AMM1 TT 25 ºC reaction at 1min. The only consistent temperature dependence of guanine reactivity was the 0 ºC reactions for AMM1 and AMM1 TT, which always had the lowest reactivity. When the AMM2 guanine reactivity of AMM1 and AMM1 TT was

compared for each temperature, AMM2 duplexed with AMM1 TT was generally more reactive than AMM1 for each respective temperature.

3.11b $KMnO_4$ Reactions with AMM2

Unlike the DMS reaction for AMM2, the $KMnO_4$ reactions showed a clear difference in reactivity of AMM2 thymines duplexed with the mutated AMM1TT strand versus AMM1. According to the polyacrylamide gel in Figure 3.19, AMM2 duplexed with AMM1 TT was substantially more reactive than AMM2 duplexed with AMM1. This observation was noticeable for T 1, whose gel bands darkened from 0 ºC at 2 min to 37 ºC at 6 min. The 37 ºC reactions for AMM2 duplexed with AMM1 TT had dark bands, indicating substantial base reactivity.

The general trends of thymine reactivity was that reactions of AMM2 duplexed with AMM1 TT were more reactive towards the to $KMnO_4$ reagent than AMM2 duplexed with AMM1 (Figure 3.20). Also, the reactions showed clear temperature dependence and thymine base reactivity increased with increasing temperature. Most thymine reactions increased reactivity with greater time with the exception of the AMM1 TT 37 ºC reaction at 4 min for T3, T4, and T5, which was greater in base reactivity than the same reaction at 6 min.

For each quantitated thymine base reactivity, AMM2 duplexed with AMM1 had very low reactivity ranging between 0-0.3% for all of the thymines. For AMM2 duplexed with AMM1 TT, the T2 and T3 had the lowest percent reactivities (0.2-2.5%), but T1, T4, and T5 had greater reactivities (0.5%-7.5%).

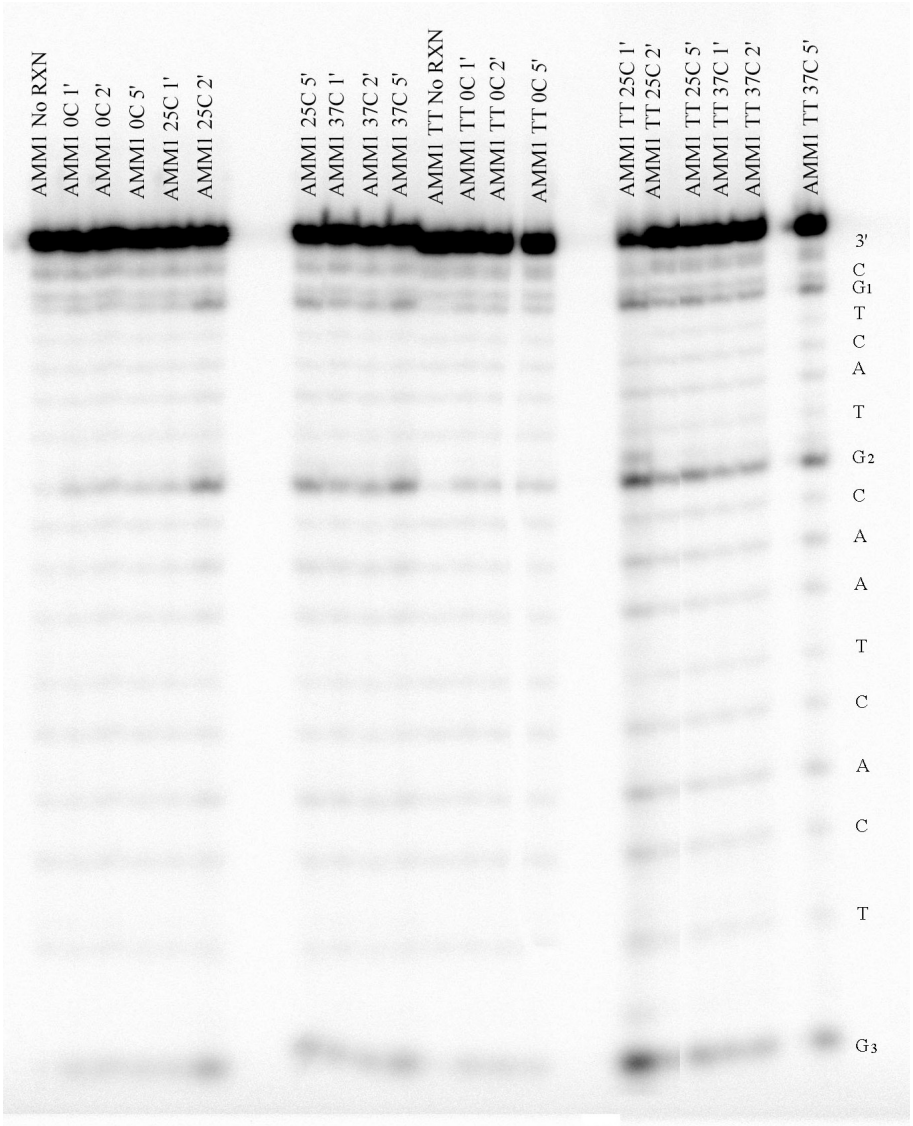


Figure 3.17 – *DMS Reactions: Radioactively Labeled AMM2 Duplexed with AMM1 and AMM1 TT*: AMM2 was the radioactive strand of interest and was duplexed to AMM1 and AMM1 TT. The DMS reactions were reacted for 2-5 min at 25 ºC and 37 ºC.

Figure 3.18 – *DMS Reactions: %Guanine Reactivity for Radioactively Labeled AMM2 Duplexed with AMM1 and AMM1TT*: These AMM2 labeled double-stranded reactions were reacted with 2.5% DMS at 0 ˚C, 25 ˚C and 37 ˚C for three time points: 1 min, 2 min, and 5 min. The AMM1 reactions are indicated in red and AMM1 TT reactions are in blue. The reactions at 0 ºC are squares, 25 ºC reactions are circles and 37 ºC reactions are triangles.

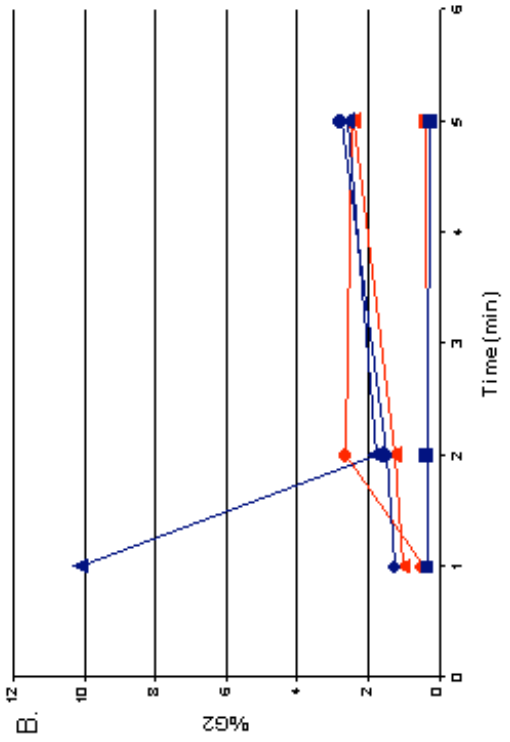


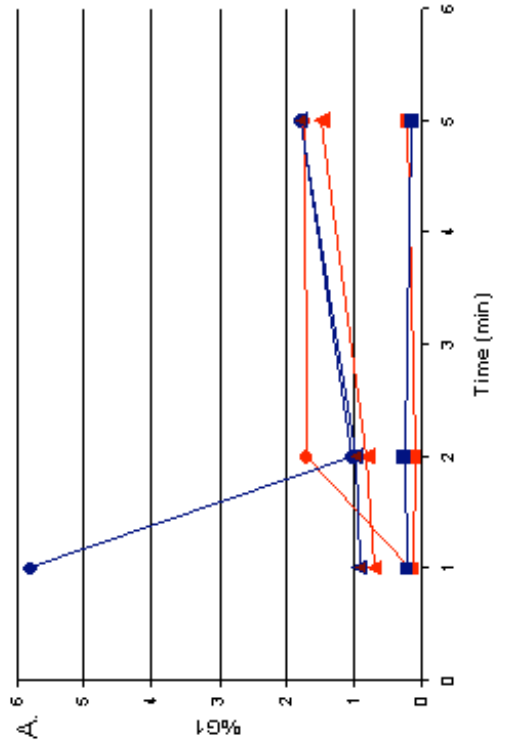


Square = 0°C Circle = 25°C Triangle = 37°C

Figure 3.18 Legend: Red = AMM1 Blue = AMM1 TT

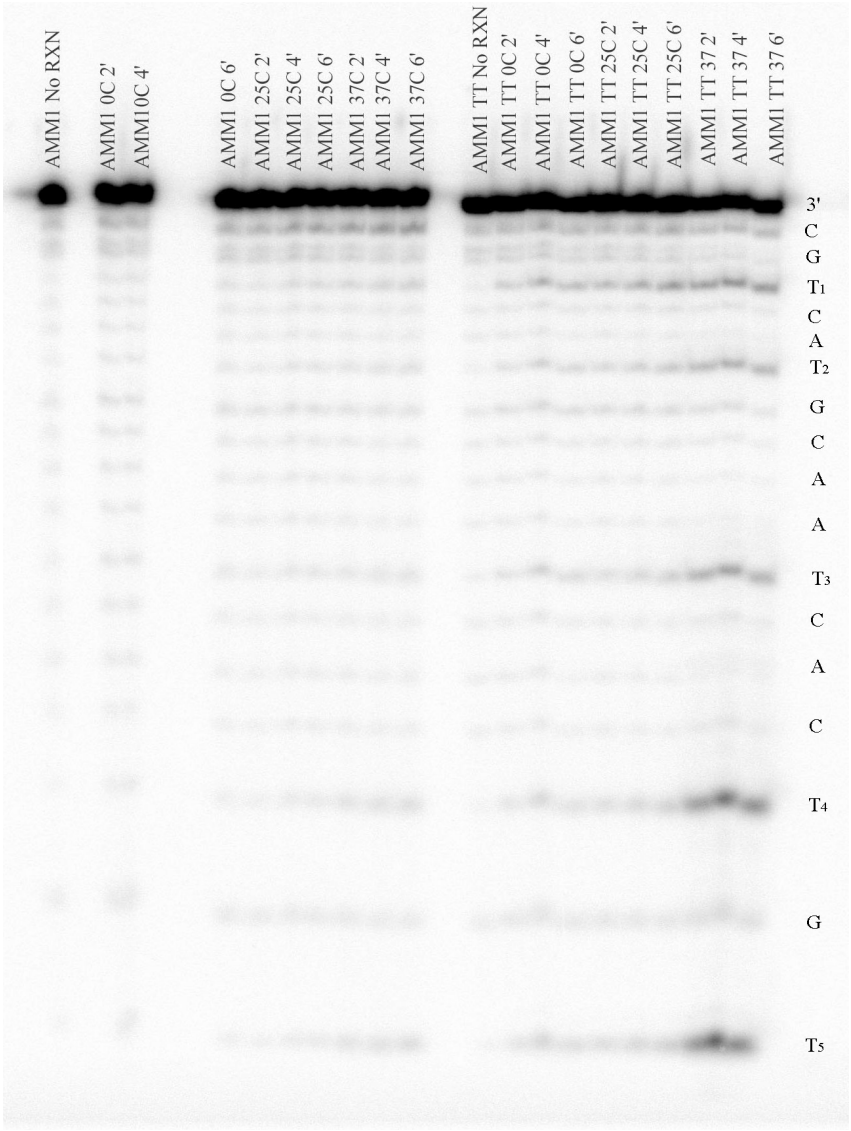


Figure 3.19 – *$KMnO_4$ Reactions: Radioactively Labeled AMM2 Duplexed with AMM1 and AMM1 TT:* AMM2 was reacted with $KMnO_4$ for 2-6 min at 0 ºC, 25 ºC and 37 ºC. The No RXN lanes were the controls the AMM1 and AMM1 TT reactions. The reactivity of the No RXN lanes are background base reactivity from piperidine cleavage and were subtracted out when determining the thymine reactivities for the reactions.

Figure 3.20 – *$KMnO_4$ Reactions: %Thymine Reactivity for AMM2 Duplexed with AMM1 and AMM1TT at 0 ˚C, 25 ˚C and 37 ˚C for 2-6 min:* These AMM2 labeled double-stranded reactions were reacted at 0 ˚C, 25 ˚C and 37 ˚C for three time points: 2 min, 4 min, and 6 min. The AMM1 reactions are indicated in red and AMM1 TT reactions are blue. The reactions at 0 ºC are squares, 25 ºC reactions are circles and 37 ºC reactions are triangles.

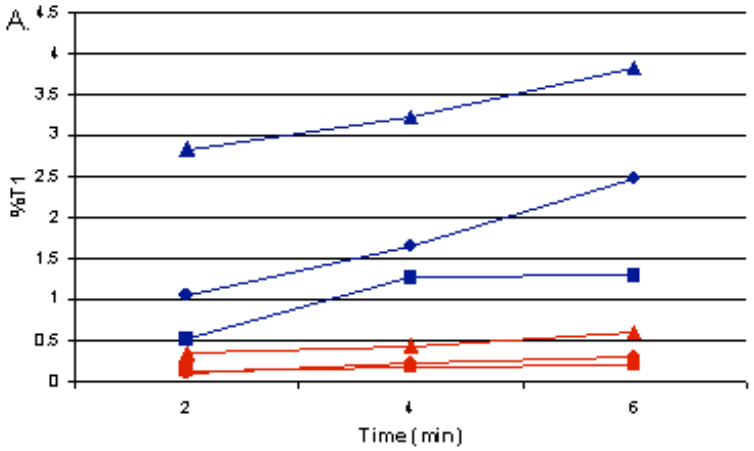


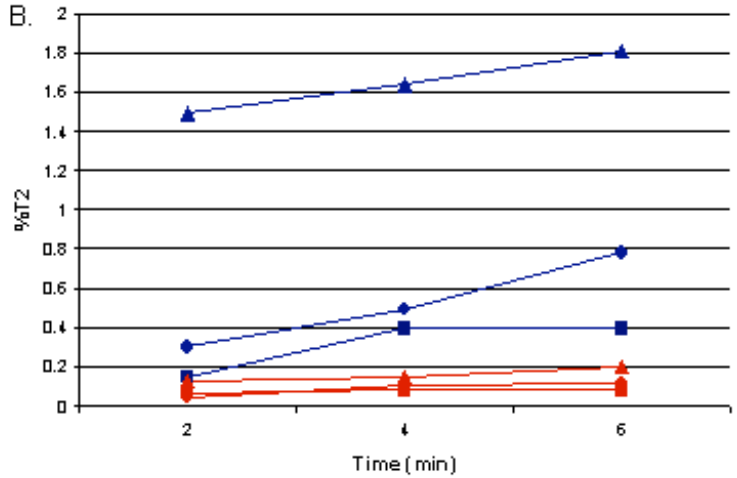


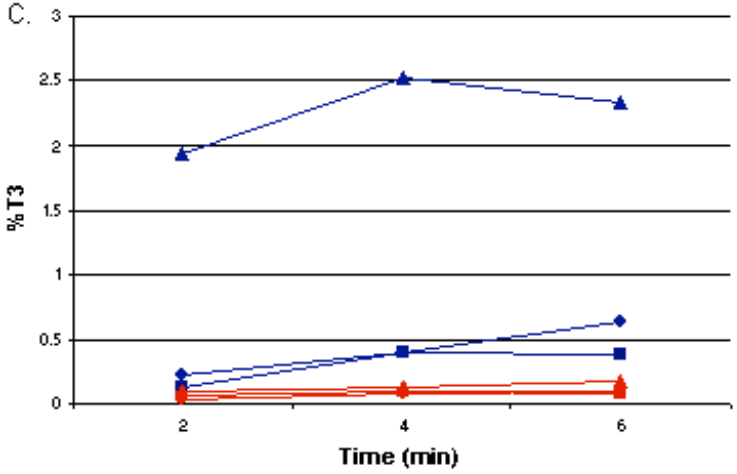


Figure 3.20 Legend: Red = AMM1 Blue = AMM1 TT Square = 0°C Circle = 25°C Triangle = 37°C

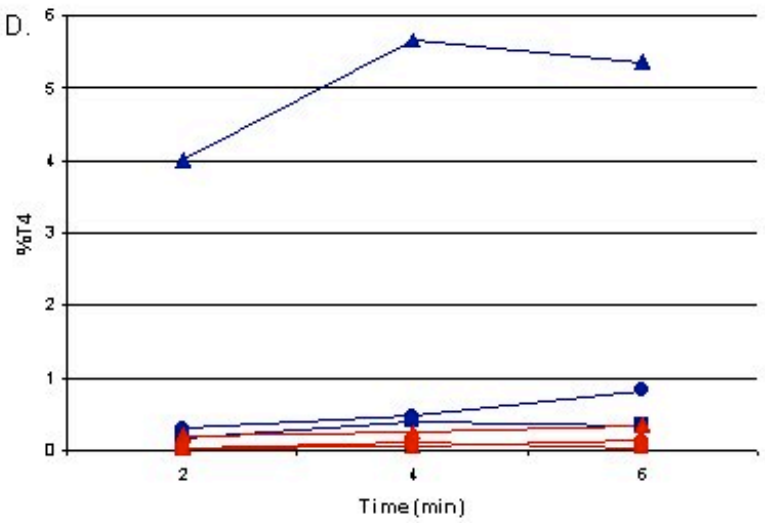


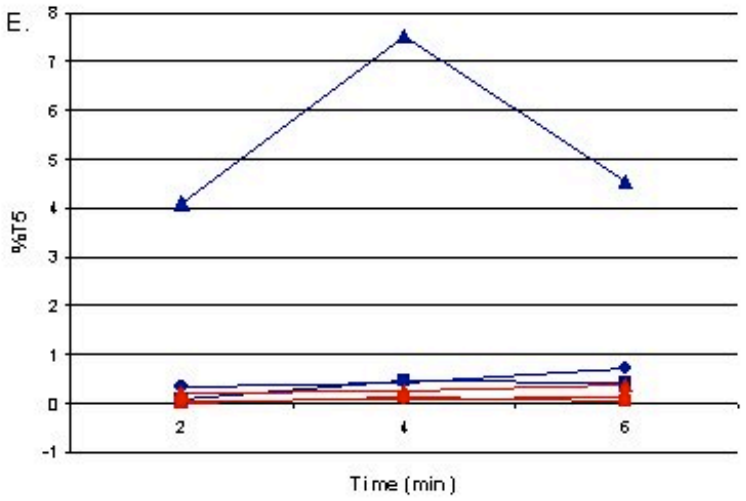


Figure 3.20 Legend: Red = AMM1 Blue = AMM1 TT Square = 0°C Circle = 25°C Triangle = 37°C

# Chapter 4 – Discussion

## 4.1 Thymine Dimer Verification

The first step was to prepare and characterize the thymine dimer according to the literature. The HPLC characterization of AMM1 TT, mass examinations of AMM1 and AMM1 TT, cycloreversal test, and T4 DNA polymerase reaction verified that the UV reaction was successful and a thymine dimer was indeed created. According to past thymine dimer HPLC studies, the thymine dimer is expected to elute before the unmodified DNA strand, and our data followed the expected trend (Douki *et al.*, 2000). The elution times of AMM1 (18.5 min) and AMM1TT (20 min) were very close to each other because the only difference between AMM1 and AMM1TT strands was the saturation of two C5, C6 double bonds of the adjacent thymines.

The AMM1 TT yields were 7.7% and 15.6% for two separate thymine dimer synthesis reactions. The yields were low because the dimer synthesis could not go to completion because thymine dimer synthesis is in equilibrium with unbound thymines. In addition, the eluted AMM1 TT was separated from AMM1 using reversed-phase HPLC, which added to the loss of AMM1 TT through purification. However, most of the AMM1 TT was needed for labeling reactions and those reactions only required DNA amounts on the micromole scale. So despite the low amounts of synthesized dimer, the yields were adequate to explore

the dimer structure. This is important for examining other lesions in the future because many are expensive, difficult to synthesize, or are rare and unstable.

The HPLC chromatograph of the cycloreversal of AMM1 TT strand gave further proof that the cyclobutane ring of the thymine dimer mutation is in equilibrium with normal thymine bases. A dose of UV light turns two adjacent thymines into a thymine dimer and another dose of UV can revert the thymine dimer back to its original unmodified state, which can be seen back in Figure 3.4c. The hump in the cycloreverted chromatograph at 18.5 min was the remnant of the AMM1 TT peak that was reconverted into the AMM1 peak at 19.6 min. The amplification of intensity of the AMM1 peak indicated an increased cycloreversion into AMM1. This process indicated that AMM1TT synthesis is a reversible reaction.

The mass spectrometry results verified that the AMM1 TT strand was not disrupted by oxidative cleavage. Oxygen was purged from the reaction container that held the AMM1 solution by the freeze-pump-thaw method. However, the effectiveness of this procedure could not be tested until AMM1 was reacted under UV light and then the mass of the synthesized AMM1 TT was determined. The ESI mass spectra proved that the sugar-phosphate backbone was not oxidized because the synthesized AMM1 TT had the same mass as the unreacted AMM1, 5857 g.

T4 DNA polymerase reaction gave significant verification that the two adjacent thymines dimerized because the enzyme stopped cleaving only in the

AMM1 TT sequence at T1, which was only three base pairs before the two adjacent thymines located in the center of the DNA strand. T4 polymerase did not stop directly before the thymine dimer mutation because the enzyme is 112,000 Daltons and most likely stopped once it contacted the thymine dimer lesion, which was several base pairs before the lesion (Panet *et al.*, 1973). The combination of the size of the T4 DNA polymerase and the kinked backbone of the mutant DNA could have blocked the enzyme from cleaving at the thymine dimer.

Research on the thymine dimer by Park *et al*. has determined that the thymine dimer bends the DNA backbone at approximately a 30-degree angle due to the formation of the cyclobutane ring, which forces the thymines of the dimer closer together. The bending of the DNA helical axis strains hydrogen bonding of bases around the thymine dimer by widening the major groove and narrowing the minor groove (Park *et al*., 2002). The bases close to the thymine dimer could have had their hydrogen bonding altered enough for the T4 DNA polymerase to terminate its 3'-5' exonuclease activity prematurely.

## 4.2 Maxam-Gilbert Purine Reactions

The Maxam-Gilbert purine (G+A) reaction uses piperidine formidate to create abasic sites at adenine and guanine bases. The main difference in using piperidine formidate for a sequencing reaction versus a chemical probe is the DNA structure used for the reaction. For sequencing reactions, the DNA structure

does not need to be conserved so the reactions are done on single strand DNA. However, for probing purposes, the DNA structure needed to be intact and in its double-stranded form. Therefore, DNA reactions were suspended in tris buffer at pH = 7.4 (1X TE) to attempt to retain the double-stranded form of DNA. However, neither the adenines nor guanines had much reactivity towards piperidine formidate with the percent base reactivities ranging approximately between –1% and 1.5% for guanines and 0-1% for adenines. The negative percent reactivities were caused by the subtraction of the control base reactivities from the reaction base reactivities. The experimental error indicated that the control reactions that lack the addition of the piperidine formidate reagent had the same magnitude as the reactions with piperidine formidate.

For the rest of the guanines there was no clear overall preference in base reactivity between AMM1 and AMM1TT, which all had overlaid percent base reactivities. When examining the damage yield at each temperature, AMM1 TT had greater guanine reactivity than AMM1 at their respective temperatures and the same trend followed for the adenines as well. The overall guanine damage yield had an almost indistinguishable increase in reactivity over time for most of the guanine reactions, which indicated that the reagent was not reacting much with the DNA substrates. The averaged guanine and adenine reactivities had large error bars according the graphed data because the signals of the Maxam-Gilbert reactions were so low.

The low signal in base reactivity was puzzling because according to the inherent instability of DNA in the presence of acid, the purines should have reacted readily with piperidine formidate, which has a pH at approximately 2. Piperidine formidate acts as a general acid to protonate N7 of the purine ring. The protonation makes the base unstable and causes it to break its glycosidic bond, breaking the base off of the sugar. Even double-stranded DNA should be accessible to protonation of N7 because that nitrogen is not involved in hydrogen bonding. In addition, if the thymine dimer was affecting the stability of the bases surrounding the mutation, then those bases could have been more accessible to solution, which would allow the acid to more easily attack the AMM1 TT purines. However, this expected result did not occur and the signal was low in the presence of piperidine formidate.

The initial hypothesis for the lack of purine base reactivity was that either the 1X TE buffer was inhibiting the reaction or the reagent was not reactive towards the strand. To increase the percent base reactivity, new reagents were tested with the AMM1 strand, and the 10% formic acid reagent produced the most intense purine bands on polyacrylamide gel and was more acidic than piperidine formidate at pH = 0-1. When examining the quantitated base reactivity from the gel bands, the double and single-stranded AMM1 percent guanine and adenine percent reactivity had a minimal preference for reactions in water over the buffer reactions. This lack of significant increase in the base reactivity signal for the water reactions versus buffer reactions revealed that the reagent was not inhibiting

the reaction. The purine reactions for this gel had overlaid percent base reactivities so no clear correlation of reactivity preference between single-strand versus double strand base reactivity could be made. This observation was particularly puzzling because lack of steric hindrance should have made N7 of the purines more accessible to solution and, thus, more accessible to the formic acid reagent. Instead, the similarity between double and single strand reactions probably indicates that in the presence of such a strong acid, the structural integrity of the DNA is lost. In a pH of 0-1, the structural integrity of the DNA double helix is most likely altered because the N1, N2, and N7 are protonated for adenine (pKa = 3.9 N1, 2.3 N3, 2.3 N7, and 10.2 N9) and N7 and N3 are protonated for guanine (pKa = 3.6 N7, 1.1 N3, 9.6 N1, and 10 N9) (Rogstad *et al*., 2003). The protonation of N1 on adenine would affect base pairing because N1 is involved in hydrogen bonding with thymine. A disruption in structural integrity should have increased purine reactivity because the DNA structure would be unstable. Therefore, the lack of signal for Maxam-Gilbert G+A reagents is still unclear. All of the reactions increased in percent base reactivity over time, but the percent increase was almost negligible because it was so small. Even when the reactions were run for a longer time, the base reactivity did not increase much. Further investigation of this reaction could lead to a solution on the low signal of piperidine formidate. Even though this reaction did not prove to be a useful probe, there were results that indicated that according to each reaction temperature, AMM1 TT was more reactive than AMM1.

4.3 Maxam-Gilbert Pyrimidine Reactions

In the Maxam-Gilbert pyrimidine (C+T) reactions, the hydrazine reagent (pH = 14) attacks the C5, C6 double bond of the pyrimidine, and the addition of pyridine cleaves the DNA strand at the pyrimidine that it attacked. At a pH of 14, N3 of both cytosine and thymine are deprotonated (NSF, 2003). Like the Maxam-Gilbert G+A reactions, the hydrazine was not reactive towards double-stranded DNA, even in the presence of a thymine dimer mutation. However, unlike the Maxam-Gilbert G+A reagent, hydrazine could have been unable to react with the DNA double strands of AMM1 and AMM1 TT due to steric hindrance. The hydrazine reagent could have been unable to insert itself to react with the C5, C6 double bond while the DNA was double-stranded. The lack of reactivity could also indicate that for the AMM1 TT strand when in double helical form, the bases near the thymine dimer had intact hydrogen bonding. If the thymine dimer caused the bases around it to destabilize into a single strand region due to the base pair hydrogen bonding strain, then hydrazine would have shown reactivity towards the pyrimidines near the thymine dimer mutation. However, these assumptions are hypothetical because the gel could not be quantitated into percent base reactivities because the Maxam-Gilbert C+T reactions produced low intensity blurred gel bands. The Maxam-Gilbert C+T reaction was not a useful probe for double-stranded AMM1 and AMM1 TT due to the inability to quantitate gel band intensity. Therefore, another reagent, potassium

permanganate, which attacks thymines by a different mechanism, was tested as a DNA probe.

## 4.4 Dimethyl Sulfate Reactions

In comparison to the Maxam-Gilbert G+A reaction, DMS reactions had greater reactivity with guanines. AMM1 and AMM1 TT guanines intensity did not correlate with temperature and time because some data points that decreased and others increased over time. AMM1 tended to be the more reactive sequence towards DMS, but it was an inconsistent trend. For guanines closer to the 5' end of AMM1 and AMM1 TT, double-stranded reactions were more reactive that the single-stranded reactions; and for guanines closer to the 3' end, the trend was the exact opposite. This trend indicated that DMS could react more readily with double-stranded or single-stranded DNA depending on the location of the guanine in the DNA sequence. In contrast, these trends could also signify that DMS has no clear preference for single-stranded DNA versus double-stranded DNA. The overlaying of percent reactivities and large standard deviations for AMM1 and AMM1 TT suggested that DMS did not have a preference to react with thymine dimer-containing DNA versus unmutated DNA.

The lack of preference of DMS to react with either AMM1 versus AMM1 TT could be a result of the mechanistic pathway in which DMS attack guanines. DMS reacts in the major groove of DNA at N7 of the guanine. DMS attacks the N7 at its lone pair of electrons that protrude from the nitrogen parallel to the base.

This mode of methylation could be insensitive to the DNA structural destabilization by a thymine dimer because the N7 could be as easily accessible for putatively "open" destabilized thymine dimer-containing DNA as normal "closed" B-form DNA. DMS is a good reagent for DNA because it produced a stronger percent base reactivity signal than the Maxam-Gilbert reactions; however, DMS was not good for discerning the destabilization properties of DNA with or without a thymine dimer.

However, there have been cases where DMS has been used as a successful probe. In research by Zhilina *et al*., DMS was used to monitor triple helix formation in the HER-2/neu oncogene, which has two polypurine tracks that can for a triplex with another strand. DMS was used to determine the accessibility of the N7 position of guanines. Protection from DMS methylation due to the Hoogsteen bonds in the triplex decreased the reactivity of DMS at the N7 of guanine bases (Zhilina *et al.*, 2004). In this particular case, DMS could successfully discriminate differences in DNA structure because of the protection from methylation at N7 of guanines. For my research, the structural alteration did not inhibit DMS accessibility at N7 because the mutation was a thymine dimer. Thus, the similarity in reactivity of AMM1 and AMM1 TT towards DMS could indicate that even though the thymine dimer is altering the overall structure of DNA by kinking the backbone, the structural differences do not have enough of a localized affect on the structural integrity of the N7 of guanine to affect DMS methylation.

4.5 Potassium Permanganate Reactions

The $KMnO_4$ reagent showed promise as a DNA base probe because this reaction produced significant differences in thymine base reactivity in unmodified DNA versus thymine dimer-containing DNA. The thymines flanking the thymine dimer of the AMM1 TT strand had greater percent reactivity than in AMM1. In the AMM1 strand, T1 barely reacted in AMM1; however, T1 in the AMM1 TT sequence reacted substantially with increasing time and temperature, which was likely due to its position near the thymine dimer. The destabilization of the hydrogen bonding network of the DNA structure caused by the 30° angle kink in the structure from the thymine dimer could have increased $KMnO_4$ reactivity for T1 and T4.

For T1 and T4, the AMM1 and AMM1 TT single-stranded reactions were more reactive than their corresponding double-stranded reactions only at their respective times and temperatures. This result indicated that the reactivity of $KMnO_4$ was directly related to the amount of steric hindrance in its substrate due to its mechanistic attack of the C5, C6 double bond. In the first step of the reaction, one of the double bonds of permanganate attacks either the C5 or C6 carbon, coming in from the top of the thymine base. Less steric hindrance allowed the $KMnO_4$ reagent to react more readily with the single-stranded DNA than more sterically hindered double-stranded DNA.

T4 reactivity deviated from T1 reactivity at the double-stranded AMM1 TT reaction at 37 ºC (Figure 3.16). This double-stranded reaction was greater in

reactivity than its single-stranded counterpart. In fact, this reaction was comparable in percent thymine reactivity to the single-stranded AMM1 reaction at 37 ºC. For T4 at 37 ºC, double-stranded AMM1 TT reacted like single-stranded DNA. This result could indicate that the destabilization of DNA structure attributed to the thymine dimer was causing DNA unwinding at 37 ºC. AMM1 TT could be partially melted at 37 ºC, allowing $KMnO_4$ to react with double-stranded AMM1 TT as if it was single-stranded. The differences between the reactivity of T1 and T4 on the AMM1 TT strand were initially thought to be related to their position in relation to the dimer mutation. When examining the sequence (Figure 2.1), T1 is located three base pairs up from the dimer in the 3' direction and T4 is four base pairs down from the dimer in the 5' direction. T1 and T4 are nearly symmetrically flanking the dimer in the 3' and 5' direction. Possibly the greater reactivity for T4 could indicate that the thymine dimer has a greater destabilizing effect on bases near the 5' end than for the 3' end. However, more repetitions of these $KMnO_4$ reactions would need to be run to determine if this is a verifiable statement about the preference of DNA destabilization by the thymine dimer.

Thymines T2 and T3 were *less* reactive within the AMM1 TT strand than in the AMM1 strand. T2 and T3 of AMM1 TT were unresponsive to $KMnO_4$ because their C5, C6 double bonds were involved in the cyclobutane ring and, thus, were unable to react with $KMnO_4$. When the thymines were not in their dimerized state, they were more open to reaction with the $KMnO_4$, which made

T2 and T3 in AMM1 more reactive than the T2 and T3 in AMM1 TT. The single strand reactions for T2 and T3 were also more reactive than the double strand reactions for both AMM1 and AMM1 TT due to base accessibility in single-stranded DNA.

Like DMS, $KMnO_4$ has been used as a probe for DNA structure alterations. In the research by Ramaiah *et al.*, potassium permanganate was used to analyze thymine dimer direct repair by photolyase (Ramaiah *et al.*, 1998). Since thymine dimers do not have an available C5, C6 double bond, due to the formation of the cyclobutane ring, the researchers determined that $KMnO_4$ would not react or react in a lower magnitude and more slowly than with an unmodified thymines. The difference in reactivity between normal thymines and a thymine dimer allowed $KMnO_4$ to be used in detection of thymine dimer repair in DNA oligonucleotides. In effect, my research verified that T2 and T3 of the thymine dimer lesion in AMM1 TT reacts less with $KMnO_4$ that unmodified thymines.

## 4.6. AMM2 Dimethyl Sulfate and Potassium Permanganate Reactions

### 4.6a. DMS Reactions with AMM2

When probed with DMS, AMM2 duplexed with AMM1 and AMM1 TT had similar trends of guanine reactivity as the previous DMS reactions with labeled AMM1 and AMM1 TT strands (Figure 3.18). Guanines 1-3 had reactivity well above the control reactions, but all of the percent guanine reactivities for the different sequences and temperature reactions overlaid each other. The guanine

reactions at 0 ºC AMM2 duplexed with AMM1 and AMM1 TT consistently had the lowest reactivity, which indicated that DMS kinetically reacts more slowly at cold temperatures. In contrast to the past DMS reactions, AMM2 duplexed with AMM1 TT was generally more reactive than AMM1 for each respective temperature. This result suggested that DMS protonation could distinguish between mutated and unmutated DNA only within each respective temperature. The kinking of the DNA backbone could have made the complementary strand's bases more accessible to solution and, therefore, more reactive to DMS. However, more DMS reactions of AMM2 would have to be conducted to verify this observation.

4.6b. $KMnO_4$ Reactions with AMM2

Unlike the DMS reaction for AMM2, the $KMnO_4$ reactions showed a clear difference in reactivity of AMM2 thymines duplexed with the mutated AMM1TT strand versus AMM1. AMM2 duplexed with AMM1 TT was more reactive towards the to $KMnO_4$ reagent than AMM2 duplexed with AMM1 at every temperature. Also, the reactions showed clear temperature and time dependence with thymine base reactivity increasing with time and temperature. The increase in thymine reactivity was significantly greater for AMM2 duplexed with AMM1 TT, which suggested that the strained hydrogen bonds due to the thymine dimer lesion could have been weakened at higher temperatures. The low percentages of

thymine reactivity for AMM2 duplexed suggested that and unmutated strand had no effect on the reactivity of its complementary bases to $KMnO_4$.

4.7 Molecular Probe Reactions in comparison to previous thymine dimer research

Past research on DNA base mutations implemented various techniques to attempt to determine the extent of destabilization to the DNA structure. Using X-Ray crystallography, Park *et al.* determined that thymine dimer-containing DNA decamer had an overall helical axis bend of 30° toward the major groove and a 9° unwinding of the helix (Park *et al.*, 2002). Within the local structure of the dimer DNA, structural alterations included pinching at the minor groove at the 3′ side of the lesion, -17.8° tilt angle of the complementary adenine of the thymine dimer on the 5' side, widening of the major and minor grooves in the 3′ and 5′ direction of the CPD. Park *et al.* hypothesized that these destabilizing structural deviations from B-form DNA could allow for DNA repair enzyme recognition. The binding affinities of the repair enzymes for thymine dimer DNA could be related to DNA unwinding or kinking. In context of the $KMnO_4$ reaction, T1 and T4 of the AMM1 TT sequence (Figure 3.16) and T1, T4, and T5 for AMM2 (Figure 3.20) were the most reactive bases and could possibly serve as sites of unwinding within the sequence, allowing $KMnO_4$ to react more easily with the destabilized substrate.

Using NMR, Taylor *et al.* studied the chemical shifts of a DNA octamer, a decamer containing a *cis-syn* dimer and another containing a *trans-syn* dimer.

The data suggested that the helix structure was more perturbed on the 3' side of the *cis-syn* dimer and on the 5' side of the *trans-syn* dimer (Taylor *et al.*, 1990). Similar to thymine dimer crystallography studies, NMR data gave an overview of the structural destabilization. Large upfield imino proton shifts of the *cis-syn* thymine dimer octamer suggested that hydrogen bonding was reduced at the complementary adenines (Taylor *et al.*, 1990). However, ring current effects of the bases could have caused the upfield imino shifts as well; therefore this data alone could not verify hydrogen-bonding reduction at the adenines. While NMR is a useful tool for studying the destabilization of a thymine dimer, however, NMR mainly studies short nucleotides that have inherently very low melting points because larger strands of DNA produce spectra that are too complicated to be fully resolved. Therefore, it would be difficult to determine base opening and accessibility in long pieces of DNA. Another difficulty in using NMR is the requirement of a large amount of synthesized mutant DNA in order to run NMR tests. Thymine dimer synthesis produces low yields and a lot of dimer DNA would be required to be synthesized prior to NMR experimentation. The usefulness of molecular probing is that DNA amounts in the range of nanomoles could be used to assay base-specific destabilization.

Another common method of examining DNA lesions has been melting point determination. DNA that has a thymine dimer lesion has decreased melting temperature, which indicates destabilization of the overall DNA structure. The Taylor group determined the melting temperature of an unmodified DNA decamer

duplex (64 °C) and a DNA decamer duplex containing a *cis-syn* thymine dimer (55 °C) (Taylor *et al.*, 1990). This 9 °C drop in temperature was considered to be only a slight perturbation of structure stability. In addition, the Lingbeck group studied the thermodynamic properties and melting points of a *cis-syn* thymine at two adjacent thymines for one strand and at two thymines of a TCT sequence, which created a base pair bulge in the DNA. In relation to their respective unmodified strands, the adjacent dimer only decreased the free energy of duplex formation by 1.5 kcal/mol and the $T_m$ by 6 ºC. The nonadjacent dimer was much more disruptive to the double helical structure($\Delta\Delta G$ = 4.0 kcal and $\Delta T_m$ = -17 ºC) (Lingbeck and Taylor, 1999). The nonadjacent CPD was the more destabilizing lesion because of the formation of the cytosine base bulge in the DNA. The bending of the DNA duplex causes hydrogen-bonding strain, which decreases the melting temperature. However, for a *cis-syn* thymine dimer strand a 6-9 ºC temperature change for a thymine dimer-containing DNA strand, in thermodynamics, is considered to be a small thermodynamic alteration.

X-Ray crystallography, NMR, and thermodynamics have shown insight into the overall structure of DNA and its destabilization in the presence of a thymine dimer mutation. However, all of these experiments give little information about the structural stability of the individual bases and none give quantitative data of the base destabilization.

Potassium permanganate has proven to be the best chemical to probe duplex and single-stranded DNA structure to give quantitated data of base

destabilization, i.e. increased reactivity, of thymine dimer-containing DNA. Of all the chemical probes, $KMnO_4$ produced the greatest base reactivity signal and showed clear preference for reactivity of thymines in the dimer-containing strand in comparison to AMM1. The thymine bases surrounding the thymine dimer of the lesion strand and the complementary strand were both more reactive towards $KMnO_4$ than the unmutated AMM1 strand. The increased reactivity could indicate that the bases were more accessible to solution due to destabilization in the DNA double helical structure. The base accessibility could be a molecular signal to a scanning DNA repair enzyme that a thymine dimer lesion is near. Using molecular probes, such as $KMnO_4$ in conjunction with past research of thymine dimers could give a broader picture of how the DNA structure is altered by DNA base mutations.

## 4.8 Future Exploration

Further research of DNA base destabilization and thymine dimers will be conducted by fellow researcher, Amy Rumora. Melting temperatures will be used to determine thermodynamic parameters for AMM1 and AMM1 TT. Also, more $KMnO_4$ reactions will be done on AMM1 and AMM1 TT to further examine reproducibility of the reaction and to obtain more accurate error bars of thymine base reactivity. A new dimer strand will be examined as well to determine whether certain bases are more reactive than others in proximity to a thymine dimer lesion.

Several more chemical probes will be tested with this DNA such as DEPC and osmium tetroxide. $OsO_4$ reacts at the C5, C6 double bond of pyrimidines in the presence of tertiary amines such as pyridine (Ohshima *et al*., 1996). $OsO_4$ is also more reactive to single-stranded DNA than to double-stranded DNA. This chemical has been used as a probe to detect unpaired single-stranded DNA; and could possibly be used to probe the unwinding in double-stranded AMM1 TT.

Using a potassium permanganate probe in conjunction with the previously mentioned DNA mutation experiments would prove to be a powerful tool in examining not only the thymine dimer lesion but also to examine the base destabilization of other base lesions in an attempt to elucidate how repair enzyme find base lesions on DNA. The extent of destabilization in a DNA strand could be determined in relation to its distance from the mutation. The structural destabilization of bases near a mutation could signal to a repair enzyme that a mutation is near. Probes could also determine the effect of DNA destabilization, whether it is kinetic or thermodynamic destabilization according to temperature and time dependence of base reactivity. Chemical probes such as potassium permanganate can be used as a simple, efficient assay to quantify base destabilization for rare lesions that are difficult to synthesize.

# REFERENCES

1 Alberts, B., Bray, D., Lewis, J., Raff, M., Roberts, K., Watson, J. D. Molecular biology of the cell. 3rd ed. Garland. 1994.

2 Bloomfield, V. A., Crothers, D.M., Tinoco, I., and Hearst, J. (2000) Nucleic Acids: Structures, Properties, and Functions. University Science Books: Sausalito, CA.

3 Brown,T., Hunter,W. N., Kneale, G., Kennard,O. (1986) Molecular structure of the G:A base pair in DNA and its implications for the mechanism of transversion mutations. *Proc. Natl Acad. Sci. USA*, **83**, 2402–2406.

4 Bruice, P. Y. Organic Chemistry. Prentice-Hall, Inc. 1999.

5 Bruner, S. D., Norman, D. P. G., Verdine, G. L.. (2000) Structural basis for recognition and repair of the endogenous mutagen 8-oxoguanine in DNA. *Nature* **403**, 859-866.

6 ChemDraw. CambridgeSoft. 1986-2004.

7 Chinnapen, D. J. F. and Sen, D. (2004) A deoxyribozyme that harnesses light to repair thymine dimers in DNA. *Proc. Natl. Acad. Sci. USA*. **101**(1), 65-69.

8 David, S. (2005) How do DNA-repair enzymes find aberrant nucleotides among the myriad of normal ones? One enzyme has been caught in the act of checking for damage, providing clues to its quality-control process. *Nature* **434**, 569-570.

9 Douki, T., Court, M., Sauvaigo, S., Odin, F., Cadet, J. (2000) Formation of the Main UV-induced Thymine Dimeric Lesions within Isolated and Cellular DNA as Measured by High Performance Liquid Chromatography-Tandem Mass Spectrometry. *Journal of Biological Chemistry* **275**(16), 11678-11685.

10 Friedberg, E.C., Walker, G.C., and Siede, W. (1995) DNA Repair and Mutagenesis. ASM Press. Washington, D. C. 1-698.

11 http://www.public.asu.edu/~iangould/reallife/thymine/thymine.html

12 Lewin, B. (2000) Molecular Biology Full Edition. Virtual Text. www.ergito.com

13 Lingbeck, J. M. and Taylor, J. S. (1999) Preparation and Characterization of DNA Containing a Site-Specific Nonadjacent Cyclobutane Thymine Dimer of the Type Implicated in UV-Induced-1 Frameshift Mutagenesis. *Biochemistry* **38**, 13717-13724.

14 Maxam, A. M. and Gilbert, W. (1977) A New Method For Sequencing DNA. *Proc. Natl. Acad. Sci. USA.* **74**(2), 560-564.

15 Mees, A., Klar, T., Gnau, P., Hennecke, U., Eker, A. P. M., Carell, T. Essen, L. (2004) Crystal Structure of a Photolyase Bound to a CPD-Like DNA Lesion After in Situ Repair. *Science* **306**(5702), 1789-1793.

16 Nelson, D. and Cox, M. Lehninger Principles of Biochemistry. Fourth Ed. W. H. Freeman and Company. New York. 2004.

17 NSF: National Science Foundation Tutorial. 2003 http://dwb.unl.edu/Teacher/NSF/C08/C08Content.html

18 Nunez, Megan. (2004) Needle in a Haystack: Removing Base Lesions from DNA. Mount Holyoke College Publication.

19 Ohshima, K., Kang, S., Larson, J. E., Wells, R. D. (1996) TTA-TAA Triple Repeats in Plasmids Form a Non-H Bonded Structure. *Journal of Biological Chemistry* **271**(28), 16784-16791.

20 Park, H., Zhang, K., Ren, Y., Nadji, S., Sinha, N., Taylor, J. S., Kang C. (2002) Crystal Structure of a DNA Decamer Containing a *Cis-Syn* Thymine-Dimer. *Proc. Natl. Acad. Sci. USA* **99**, 15965.

21 Panet, A., van de Sande, J. H., Loewen, P. C., Khorana, H. G., Raae, A. J., Lillehaug, J. R., and Kleppe, K. (1973) Physical characterization and simultaneous purification of bacteriophage T4 induced polynucleotide kinase, polynucleotide ligase, and deoxyribonucleic acid polymerase. *Biochemistry* **12**, 5045-5050.

22 Ramaiah, D., Koch, T., Orum, H., Schuster, G. B. (1998) Detection of thymine [2+2] photodimer repair in DNA: selective reaction of KMnO4. *Nucleic Acids Res.*, **26**(17), 3940–3943.

23 Rogstad K. N., Jang Y. H., Sowers, L. C., Goddard, W. A. (2003) First Principles Calculations of the p$K_a$ Values and Tautomers of Isoguanine and Xanthine. *Chem. Res. Toxicol*. **16**(11), 1455-1462.

24 Rouzina, I and Bloomfield, V. A. (1999) Heat Capacity Effects on DNA Melting. *Biophysical Journal*. **77,** 3242-3251.

25 Taylor, J. S., Garrett, D. S. Brockie, I. R., Svoboda, D. L., Telser, J. (1999) $^{1}$H NMR Assignment and Melting Temperature Study of *Cis-Syn* and *Trans-Syn* Thymine Dimer Containing Duplexes of d( CGTATTATGC)*d(GCATAATACG). *Biochemistry* **29**, 8858-8866.

26 Torizawa T, Yamamoto N, Suzuki T, Nobuoka K, Komatsu Y, Morioka H, Nikaido O, Ohtsuka E, Kato K and Shimada I. (2000) DNA binding mode of the Fab fragment of a monoclonal antibody specific for cyclobutane pyrimidine dimer. *Nucleic Acids Res*. **28**(4) 944-951.

27 Zhilina Z. V., Ziemba A. J., Trent J. O., Reed M. W., Gorn V., Zhou Q., Duan W., Hurley L., Ebbinghaus S. W. (2004) Synthesis and evaluation of a triplex-forming oligonucleotide-pyrrolobenzodiazepine conjugate. *Bioconjug Chem*. **15**(6):1182-92.